(2)

POR-2032(EX)
(WT-2032)(EX)
VOLUME 1
EXTRACTED VERSION

OPERATION DOMINIC
FISH BOWL SERIES
PROJECT OFFICERS REPORT — PROJECT 6.13
RF MEASUREMENTS AND OPTICAL MEASUREMENTS — SUMMARY

J.E. Hagefstration, Project Officer

Army Missile Command
Redstone Arsenal, Alabama

and personnel of:

Radio Corporation of America
Missile and Surface Radar Division
Moorestown, New Jersey

and

Barnes Engineering Company
30 Commerce Road
Stamford, Connecticut

15 May 1964

NOTICE:
This is an extract of POR-2032 (WT-2032), Volume 1, Operation DOMINIC, Fish Bowl Series, Project Officers Report, Project 6.13.

Extracted version prepared for
Director
DEFENSE NUCLEAR AGENCY
Washington, DC 20305-1000

1 April 1985

Destroy this report when it is no longer needed. Do not return to sender.

PLEASE NOTIFY THE DEFENSE NUCLEAR AGENCY, ATTN: STTI, WASHINGTON, DC 20305-1000, IF YOUR ADDRESS IS INCORRECT, IF YOU WISH IT DELETED FROM THE DISTRIBUTION LIST, OR IF THE ADDRESSEE IS NO LONGER EMPLOYED BY YOUR ORGANIZATION.

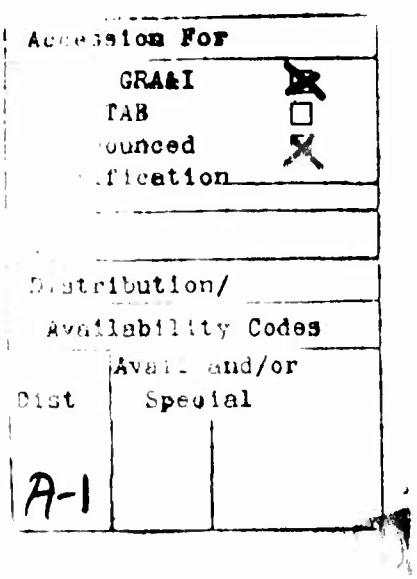

UNCLASSIFIED
SECURITY CLASSIFICATION OF THIS PAGE

AD-A275287

REPORT DOCUMENTATION PAGE

Form Approved
OMB No. 0704-0188
Exp. Date: Jun 30, 1986

1a. REPORT SECURITY CLASSIFICATION UNCLASSIFIED	1b. RESTRICTIVE MARKINGS
2a. SECURITY CLASSIFICATION AUTHORITY	3. DISTRIBUTION/AVAILABILITY OF REPORT Approved for public release; distribution is unlimited.
2b. DECLASSIFICATION/DOWNGRADING SCHEDULE	
4. PERFORMING ORGANIZATION REPORT NUMBER(S)	5. MONITORING ORGANIZATION REPORT NUMBER(S) POR-2032(EX) (WT-2032(EX))
6a. NAME OF PERFORMING ORGANIZATION 1-Radio Corp. of America 2-Barnes Engineering Co. 6b. OFFICE SYMBOL (If applicable)	7a. NAME OF MONITORING ORGANIZATION Defense Atomic Support Agency
6c. ADDRESS (City, State, and ZIP Code) 1-Moorestown, NJ 2-Stamford, CT	7b. ADDRESS (City, State, and ZIP Code) Washington, DC
8a. NAME OF FUNDING/SPONSORING ORGANIZATION 8b. OFFICE SYMBOL (If applicable)	9. PROCUREMENT INSTRUMENT IDENTIFICATION NUMBER
8c. ADDRESS (City, State, and ZIP Code)	10. SOURCE OF FUNDING NUMBERS PROGRAM ELEMENT NO / PROJECT NO / TASK NO / WORK UNIT ACCESSION NO.

11. TITLE (Include Security Classification)
OPERATION DOMINIC, FISH BOWL SERIES, PROJECT OFFICERS REPORT - PROJECT 6.13, RF MEASUREMENTS AND OPTICAL MEASUREMENTS--SUMMARY, EXTRACTED VERSION

12. PERSONAL AUTHOR(S)
J.E. Hagefstration

13a. TYPE OF REPORT	13b. TIME COVERED	14. DATE OF REPORT (Year, Month, Day)	15. PAGE COUNT
	FROM _____ TO _____	1964, May 15	140

16. SUPPLEMENTARY NOTATION This report has had sensitive military information removed in order to provide an unclassified version for unlimited distribution. The work was performed by the Defense Nuclear Agency in support of the DoD Nuclear Test Personnel Review Program.

17 COSATI CODES		
FIELD	GROUP	SUB-GROUP
18	3	
17	4	

18. SUBJECT TERMS (Continue on reverse if necessary and identify by block number)
Dominic, Fish Bowl, Auroras, Ionospheric Bursts, Electromagnetic Radiation, Star Fish Check Mate, Blue Gill Triple Prime, Tight Rope, King Fish

19. ABSTRACT (Continue on reverse if necessary and identify by block number)
The primary objective of this project was to make RF measurements to determine the amount of radar refractive jitter present in a nuclear burst environment. The secondary objectives were: (1) measurement of electron line density; (2) investigation of radar clutter; (3) measurement of RF noise produced at one radar frequency; (4) measurements of absorption over a wide portion of the RF spectrum; (5) study of the early time effects of the fireball on radar measurements at several frequencies; (6) measurement of fireball reflection at early times (Blue Gill); and, (7) measurements of dissociated region reflectivity (Star Fish Prime). Optical measurements were made to determine: (1) damage to direct optical viewing systems, and (2) saturation and blanking of instrumentation viewing the burst region. Additional measurements, in support of other projects, were accomplished.

20. DISTRIBUTION/AVAILABILITY OF ABSTRACT	21. ABSTRACT SECURITY CLASSIFICATION
☒ UNCLASSIFIED/UNLIMITED ☐ SAME AS RPT ☐ DTIC USERS	UNCLASSIFIED
22a. NAME OF RESPONSIBLE INDIVIDUAL Betty L. Fox	22b. TELEPHONE (Include Area Code) 202-325-7042 / 22c. OFFICE SYMBOL STTI

DD FORM 1473, 84 MAR 83 APR edition may be used until exhausted
All other editions are obsolete

SECURITY CLASSIFICATION OF THIS PAGE
UNCLASSIFIED

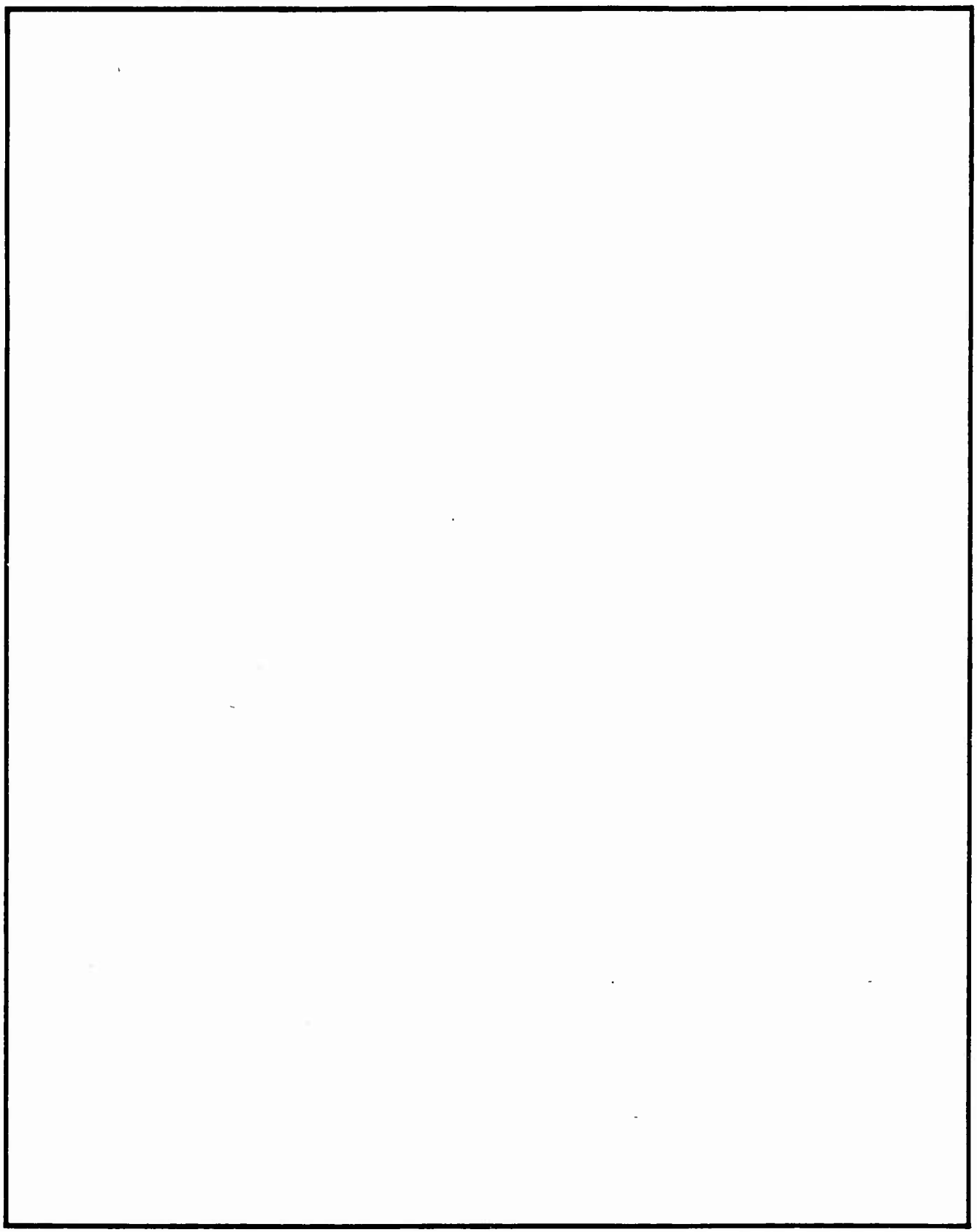

FOREWORD

Classified material has been removed in order to make the information available on an unclassified, open publication basis, to any interested parties. The effort to declassify this report has been accomplished specifically to support the Department of Defense Nuclear Test Personnel Review (NTPR) Program. The objective is to facilitate studies of the low levels of radiation received by some individuals during the atmospheric nuclear test program by making as much information as possible available to all interested parties.

The material which has been deleted is either currently classified as Restricted Data or Formerly Restricted Data under the provisions of the Atomic Energy Act of 1954 (as amended), or is National Security Information, or has been determined to be critical military information which could reveal system or equipment vulnerabilities and is, therefore, not appropriate for open publication.

The Defense Nuclear Agency (DNA) believes that though all classified material has been deleted, the report accurately portrays the contents of the original. DNA also believes that the deleted material is of little or no significance to studies into the amounts, or types, of radiation received by any individuals during the atmospheric nuclear test program.

ABSTRACT

The primary objective of the Project 6.13 DAMP ship (USAS American Mariner) participation in the Fish Bowl Series was to make RF measurements to determine the amount of radar refractive jitter present in a nuclear burst environment. The secondary objectives were: (1) measurement of electron line density, (2) investigation of radar clutter, (3) measurement of RF noise produced at one radar frequency, (4) measurement of absorption over a wide portion of the RF spectrum, (5) study of the early time effects of the fireball on radar measurements at several frequencies, (6) measurement of fireball reflection at early times (Blue Gill), and (7) measurement of dissociated region reflectivity (Star Fish Prime). Optical measurements were made to determine: (1) damage to direct optical viewing systems, and (2) saturation and blanking of instrumentation viewing the burst region. Additional measurements, in support of other projects, were accomplished.

A summary of the data on the five events proves conclusively that the effects observed were both serious and of longer duration than previously suspected, but varied considerably with yield and altitude. It was demonstrated during the Blue Gill Triple Prime event that loss of precision tracking data may be incurred up to 5½ minutes after burst, due to fluctuations in the apparent angle of arrival of the target signals in the nuclear environment (angular jitter). Although, for almost every test, instantaneous single-pulse effects at H - 0 were overwhelming, the longer lasting 20- to 30-decibel attenuations observed through debris regions several minutes after burst were very significant.

These measurements are far more significant in application to a passive radar system when it is considered that they represent the one-way propagation effects of a tracked beacon target rather than passive skin track. Of even more importance in its application to the field of target discrimination is the appearance of tens of decibels of noiselike signal fluctuation occurring for periods longer than 10 seconds after burst.

This report consists of seven volumes, this volume, plus one volume for each of the five Fish Bowl events and a volume covering other selected data (see Preface).

PREFACE

This report is published in seven volumes as follows:

Volume	Title
1	RF Measurements and Optical Measurements—Summary
2	RF Measurements and Optical Measurements, Shot Star Fish Prime
3	RF Measurements and Optical Measurements, Shot Check Mate
4	RF Measurements and Optical Measurements, Shot Blue Gill Triple Prime
5	RF Measurements and Optical Measurements, Shot King Fish
6	RF Measurements and Optical Measurements, Shot Tight Rope
7	Radar, Radiometric, and Coherent Measurements

CONTENTS

PART 1

RF MEASUREMENTS (U)

J. E. Hagefstation, Project Officer

Contributors:

E. Austein
R. Bachinsky
A. Gold
R. E. Kansas
E. Phelan

Radio Corporation of America
Missile and Surface Radar Division
Moorestown, New Jersey

PART 1

RF MEASUREMENTS

CHAPTER 1

INTRODUCTION

1.1 OBJECTIVES

The primary objective of the DAMP ship (USAS American Mariner) participation in the Fish Bowl Series was to make various RF measurements to determine the amount of radar refraction jitter present in a nuclear burst environment. This is the fluctuation in the apparent angle of arrival of target signals when a high-precision monopulse tracking radar attempts to track a target through a nuclear burst environment.

The secondary objectives of DAMP participation were: (1) measurement of electron line density produced in the atmosphere as the result of a nuclear burst, (2) investigation of the radar clutter produced by a nuclear burst at various radar frequencies, (3) measurement of RF noise level produced at one radar frequency, (4) measurement of absorption over a wide portion of the RF spectrum, (5) study of the early time effects of the fireball on radar measurements at several frequencies, (6) measurement

of fireball reflection at early times (Blue Gill), and (7) measurement of dissociated region reflectivity (Star Fish Prime).

In addition to these objectives, DAMP participation was planned to provide backup information to several other projects operating in the Fish Bowl Series. These support objectives were: (1) measurement of the probe trajectory for Project 6.2, (2) recording of Thor boost telemetry for Project 9.4a, and (3) measurement of probe trajectory for Project 6.7 (Star Fish Prime only).

1.2 BACKGROUND

Project DAMP was developed to obtain scientific information in support of the design of defense systems against ballistic missiles. Any information gained on the defense problem is applicable to the complementary offensive problem of penetration. Present and proposed defense systems require high-precision target tracking in the terminal phase of the engagement. Since it is considered likely that such tracking may take place in a nuclear environment, it was essential to investigate the effect this will have on the tracking capability of a monopulse radar. Estimates by the Institute of Defense Analysis (IDA) of Advanced Research Projects Agency (ARPA)

suggest that the apparent angle of arrival of the return signal would fluctuate with sufficient amplitude and speed, due to the signal crossing regions of time-varying refractive index, so that tracking would be extremely poor or even impossible. Since there was insufficient theoretical data and no experimental data which could be used as a firm basis for deciding the question, an experimental test was indicated.

The last experimental opportunity to measure any of the parameters listed above was the Hardtack Series of tests in 1958. Unfortunately, "no direct observations of refraction of electromagnetic waves were planned for the Hardtack tests" (Reference 1). The rather incomplete series of measurements that were actually made were used as the basis for constructing this theory. This left much to be desired and needed experimental checking. The Fish Bowl tests were the first planned opportunity to make measurements on the effects of a nuclear environment on tracking radars and on other types of electromagnetic propagation.

The effective reflective characteristics and extent of the radar returns from the fireball at early times is very important from the standpoint of pencil-beam high-power operational frequency radars for defense systems.

These measurements determine engineering quantities to be used as defense system input criteria. In particular, during the rise of a well-formed fireball, as in Blue Gill Triple Prime, the fireball extent was mapped at the operational frequencies aboard the DAMP ship.

The measurement of electron line density is related to the RF propagation characteristics of the nuclear environment. Electron line density measurements are important from the defense viewpoint, because the present concept of most defense systems requires target tracking in the terminal phase. To help define the limitations of various possible tracking schemes, it is necessary to know the path attenuation that may be encountered under these circumstances. The measurement was backup to the attenuation measurements of Project 6.1. In addition, such a measurement was of interest as a means of elucidating the physics of the interaction between a nuclear burst and the atmosphere.

The measurement of clutter is necessary to determine the radar environment terminal defense systems may encounter. Clutter includes specifically the effect produced in the ionosphere in connection with the earth's magnetic field. A similar problem had been studied

with auroral clutter for early warning radars, but data pertaining to nuclear burst produced clutter was fragmentary.

RF noise is an important parameter in any radar system. The RF noise determines the minimum signal that can be detected and the maximum range of detection for a given size target. Thus, the level of RF noise produced by a nuclear burst is an important parameter in the design of terminal and other defense systems.

RF absorption measurement through the ionosphere indicated the effects of the detonations on the ionosphere. It has thus given some indication of the possible effects on high-frequency communications, and is also expected to shed some light on the physics of such phenomena.

1.3 THEORY

The theory pe[illegible] the primary objective of these tests involves calcu[illegible] the range and angle errors due to an electron distribution along the propagation path between the radar and the target. This electron distribution alters the refractive index along the propagation path. If the distribution and amount of ionization are assumed, range errors, total refractive errors, and refractive jitter errors can be calculated. However, the

assumptions are questionable and are chosen to achieve an easily calculable result. Any real situation will likely vary considerably from the assumptions made in such calculations. An additional point to keep in mind in discussing this theory is that the calculations for refractive jitter error are based on the implicit assumption that phase distortion across the wave front arriving at the receiving antenna will result in spurious error signals being generated within the radar. However, this reasoning applies to phase-sensitive tracking situations only, such as in the Azusa system which uses extended antennas. In the amplitude monopulse system used in the FPQ-4, the intensity of the wave across the antenna aperture is averaged by the radar, because the energy intercepted by the dish is reflected into the feedhorn. Phase variations in this wave front are not registered by radar. The radar is sensitive to the fluctuations in the intensity of the received signal as a function of angle off axis. Thus, if the signal actually comes from the same direction all the time, even though it may fluctuate in phase across the wave front arriving at the antenna, the radar operates so that these phase fluctuations are averaged out.

The beta electrons created by the radioactive debris of a nuclear burst are captured by the earth's magnetic field lines and channeled into cylinders aligned parallel to the field. There is strong indication that the free electron density created by the beta flux is nonuniform. The free electron density is described as being constant in each cylinder but varying from cylinder to cylinder. Such field-aligned striations can be commonly observed in the natural aurora. Any beam propagated through such a striation experiences variation in its phase across the wave front causing destruction of the angular coherence and resulting in angular scattering. This phenomenon may be caused by nonuniformity in the distribution of the debris or magnetohydrodynamic instabilities.

One result of this phenomenon is the occurrence of jitters in the apparent angle of arrival of signals at a receiver. An analogous problem in astronomy, where major fluctuations occur because of the great range to the target, contributes some uncertainty to the actual position of observed celestial objects.

When an electromagnetic signal from a moving source propagates through a medium containing charged particles, the received signal, in general, suffers a shift in

frequency from two sources: (1) doppler effect, and (2) the dispersive effects introduced by the charge density. If the initial transmitted frequency and trajectory of the source are precisely known, measurement of the received frequency can be used in principle to infer the integrated electron line density along the path of propagation. In this experiment, the transmitted signal from the Transit satellites was received to give this information. The received signal variation from Transit satellites also gave a map of the region of interest. Knowledge of this permitted an independent calculation of absorption through the medium, and this data thus served as an additional measurement in support of Project 6.1.

Assuming field-aligned cylinders of constant electron density, it is possible to calculate a frequency below which strong angular scattering will take place in the direction perpendicular to the field lines. Th[illegible]th fluctuations of electron density between the cyl[illegible] having a standard deviation sigma. The frequency can be expressed as follows:

$$f_s = \frac{K}{\sqrt{\cos\theta \sin\theta}} \frac{\sqrt{S\delta}}{C} \sigma \text{ cps} \qquad (1.1)$$

Where: θ = Angle between vertical and radar beam direction

α = Angle between magnetic field lines and radar direction

S = Altitude difference between the point the radar beam first meets a striation cylinder and the point it leaves the striation volume in meters

δ = Average diameter of a striation cylinder, meters

C = Velocity of light, 3×10^8 m/sec

σ = Standard deviation of electron density from cylinder to cylinder, electrons/cm^3

$K = 81 \times \pi \times 10^6 \frac{cm^3}{sec^2}$

Any plane wave of a frequency below the critical scatter frequency is strongly scattered in the direction perpendicular to the magnetic field lines. If the frequency is above the critical scatter frequency, the wave front is distorted, but some degree of coherence is maintained. The statistical fluctuation of the model will then produce angular fluctuation of the wave normal which is called angular jitter.

Electromagnetic waves traveling normal to the magnetic field lines are strongly reflected from the striation model. This effect has been studied to a degree in the natural phenomenon of the northern aurora. The Stanford Research Institute (SRI) and Lincoln Laboratory (LL) radars detected extensive backscatter returns from ionized regions in the Teak and Orange experiments. In general, anisotropic irregularities in electron density scatter only a small portion backward while most of the energy proceeds in the original direction. The observed aspect sensitivity of the echoes is explained by the presence of long cylindrical columns. The longer these columns are, the greater is the aspect sensitivity. The following relationship exists for backscatter from elongated field-aligned irregularities in the free electron density (Reference 2):

$$\sigma_B = \frac{2^{3/2}\pi^2}{\lambda^4_N}\left(\frac{\overline{\Delta N}}{N}\right)^2 T^2 L \exp\left[\frac{-8\pi^2 T^2}{\lambda^2}\right] \exp\left[\frac{-8\pi^2 L^2}{\lambda^2}\psi^2\right] \qquad (1.2)$$

Where: σ_B = Backscattering cross section per steradian per watt/m^2 incident, per m^3, in m^2

L = Correlation distance along axis of symmetry, meters

T = Correlation distance transverse to axis of symmetry, meters

λ = Wavelength, meters

λ_N = Plasma wavelength, meters

ψ = Angle between direction of wave travel and normal to the axis of the irregularity, radians

$\left(\frac{\overline{\Delta N}}{N}\right)^2$ = Mean square fractional deviation of electron density

On the basis of observations of the natural aurora, the cutoff frequency is above 800 Mc, and $(\Delta N/N)^2$ is about 6×10^{-4}. The cutoff frequency is controlled by the two exponential terms in Equation 1.2. To facilitate reasonable agreement between theory and experiment, the assumption $T = 0.1$ meter is made, which results in a correlation length of $L = 3.5$ meters.

Detailed comparison between experiment and theory requires more reliable estimates of the frequency dependence of the scattered power. The only available experimental data up to this time were SRI and LL measurements at 370 and 425 Mc, respectively, during Hardtack.

This brief discussion shows that essentially the same phenomenon causes both angular jitter and clutter. The

clutter measurements made by Project 6.13 were in support of Project 6.9.

A further problem involved concerns a very-high-altitude burst. It was unknown whether the debris would be contained by the earth's magnetic field, or would act as neutral particles and distribute itself without regard to the field, or if some intermediate situation would occur. Some light can be shed on this question by observing the spatial distribution of clutter. If the debris were completely magnetically contained, a major hot-spot would develop where the field through the explosion traverses the ionosphere.

In addition to the absorption information obtained from probe tracks, one method of obtaining some measure of the absorption of the ionosphere is to monitor cosmic noise level. Since this signal must traverse the ionosphere, variations in received signal level can be interpreted as variations in the absorption (and thus electron density) of the ionosphere. These measurements were made in support of Project 6.8.

CHAPTER 2

PROCEDURE

2.1 SHOT PARTICIPATION

DAMP participated in five live tests held during the Fish Bowl series. These were Star Fish Prime (1.4 Mt at 400 km), Check Mate [redacted] Blue Gill Triple Prime [redacted] King Fish [redacted] and Tight Rope [redacted] All dates and times in this report are Greenwich Mean Time.

2.2 INSTRUMENTATION

The DAMP ship brochure, RCA 0485 (Unclassified), contains a technical description of the instrumentation aboard the DAMP ship.

Instrumentation for the angular jitter experiments consisted of an AN/FPQ-4 (modified) high-precision monopulse C-band tracking radar, and a television vidicon camera mounted on a pedestal slaved to the radar. In these experiments, several probes fired from Johnston Island were tracked. Each probe carried a C-band beacon and either a set of pyrotechnic flares or a telemetry link.

The rationale governing the firing of these telemetry probes was determined by many factors, the primary factor being the following. During Shot Star Fish Prime (1.4 Mt at 400 km on 9 July 1962), the DAMP FPQ-4 radar returns from

beacon-tracked 6.13 probes showed significant deterioration for several pulses immediately following the event. Track was completely lost at subsequent times, and on one other probe at critical altitudes. To determine whether this effect is due to radiation-produced deterioration of the beacon components or due to disturbed atmospheric transmission, the output current from the beacon B+ power supply was monitored to ascertain whether or not the beacon transmitter failed. During normal receiving operation (awaiting interrogation), the beacon power supply draws 800 ma. When triggered in the normal operating mode, the beacon supply delivers 1.2 amperes. Primarily due to the lack of time available for instrumentation modifications, it was decided that only a go-no-go type of intelligence transmission was possible. The probe telemetry transmission, of the standard FM/FM variety, was equipped with a sub-carrier modulator.

If the B+ current exceeds the 800- to 1,200-ma limits of normal operation the sub-carrier modulator causes a tone shift on channel 12 or 13, which persists for the duration of the abnormal condition. This tone shift is then available after telemetry blackout recovery as a positive indication that the beacon has failed after the onset of blackout and before transmission recovery.

To shed further light on this question, probe tracking operation was changed from the beacon-only operation used on Star Fish Prime to include operation of the skin local oscillator of the radar. The history of the skin return signal was expected to give further indication of whether the medium was responsible for loss of track.

Early time fireball measurements and clutter mappimg were accomplished with a second AN/FPQ-4 (modified) C-band tracking radar plus a slaved UHF/L-band radar. (These latter two frequencies were radiated and received using a common antenna.)

RF noise level monitoring was accomplished aboard the DAMP ship by using a radiometer receiver, operating on UHF only, and used in conjunction with the UHF antenna of the slaved UHF/L-band radar.

Absorption measurements were instrumented by installing three riometers furnished by Project 6.8 aboard the ship.

Electron line density measurements were made by recording doppler and known position from Transit satellite passes. Transit navigation system receivers on the ship were used.

2.2.1 Location. All rocket probes tracked by the DAMP ship were fired from Johnston Island. The DAMP ship was located as follows: All positions are magnetic north of burst and are given with reference to the launcher. For Star Fish Prime, ship position was 356 km at 10 degrees T from Johnston Island. For Check Mate, the ship position was 190 km at 011 degrees T. For Blue Gill Triple Prime, it was 106 km at 010 degrees T. For King Fish it was 95 km at 011 degrees T. For Tight Rope, the ship position was 10 km at 011 degrees T. DAMP probe performance data is listed in Volumes 2 through 7.

2.2.2 Calibration. The basic calibration for the C-band tracking radar used for the angular jitter measurements consisted of an amplitude calibration to relate recorded signal voltage to received signal strength, and an error calibration to relate recorded error-channel voltages (azimuth and elevation) to the angle by which a tracked target is off the boresight axis. In addition, alignment of the slaved pedestal carrying the vidicon with the radar pedestal, and proper alignment and zeroing of all angle indicators, range indicators, gyros, and other auxiliary equipment was performed.

The basic calibration for the C-band radar and the UHF/L-band radar consisted of amplitude calibration in addition to all auxiliary equipment calibration as described above.

2.3 DATA

Data was recorded in several forms. The primary position information (radar range, azimuth, and elevation with respect to the ship, gyro angles) was recorded digitally on magnetic tape at a rate of 100 samples per second. The primary amplitude and angle error data were recorded on a pulse-by-pulse basis on wide-band video recorders.

Backup information on all these quantities was recorded on analog magnetic tape recorders and paper strip chart recorders. All recorders used were calibrated simultaneously.

CHAPTER 3

RESULTS AND CONCLUSIONS

3.1 BACKGROUND

The Down-range Anti-missile Measurement Program, popularly referred to as DAMP, was designed to provide ballistic missile re-entry data as a basic input to the development of ballistic missile defense systems. The program utilizes a converted, heavily instrumented, liberty-type ship, the USAS American Mariner (Figure 3.1) as its primary down-range measurement facility. The ship is supported by a planning and operations group and a data analysis laboratory containing a complete data reduction facility. The program is sponsored by the Advanced Research Projects Agency (ARPA), directed by the Army Missile Command (AMICOM), and operated by RCA. Backed with this organization, DAMP had been involved in some 60 successful re-entry measurement operations over the past five years.

One of the primary objectives of the Fish Bowl series was to obtain scientific information in support of the design of ballistic missile defense systems. Since precision tracking is essential in the design of all current defense systems concepts, it was decided in December of 1961 to apply the unique DAMP sensors and data reduction

and interpretation facilities to the task of obtaining the urgently required data discussed in this report. For the purpose of the Fish Bowl series, DAMP was designated as project 6.13, with 6.13a as RF-measurements, 6.13b as optical measurements, and 6.13c as probe design, fabrication and launching.

During the following $2^1/_2$ months, the experiments were formulated, the apparatus was developed and moved into the field, and the entire operation was planned in detail. This crash effort could not have succeeded without the close cooperation of all the participating orgainzations. In this regard, an appreciation for the support received from ARPA and AMICOM must be noted here. In particular, to both the ship's crew and the DAMP project engineers for their efforts in the design, development, and installation of new equipment and perfection of the intricate shipboard operation and also the Physical Science Laboratory of New Mexico State University for their development of the Speedball probe instrumentation and operations at Johnston Island (Figure 3.2). Additional citations belong to both the Bell Telephone Laboratory and the U. S. Army Nike-Hercules detachment for their Tight Rope operations.

3.2 OBJECTIVES

The primary objective for all tests, except Tight Rope, was to determine the amount of radar refractive glint or angular scintillation of the received phase front (jitter) present in a nuclear environment. The Tight Rope objective was to obtain a measure of the disturbed-region radar absorption.

To achieve these objectives, the project 6.13 primary experiment for all tests, except Tight Rope, consisted of a precision radar track of a beacon-carrying Speedball probe flying nearly perpendicular to the field-oriented D-layer ionization emanating from debris concentrations. The primary Tight Rope experiment consisted of a skin and beacon track of a Nike-Hercules vehicle guided on a trajectory which was to take it behind the fireball for an extended time period. The ship position in all cases was selected to be in the plane of the magnetic field lines containing the burst. The distance north of the burst was selected considering debris rise and its final location, as well as the expected clutter or radar backscatter locations. This position, the number and type of probes utilized for the time-space exploration, and other vital parameters of each test are shown on Figure 3.3.

Several types of Speedball probe instrumentations were utilized. All probes carried C-band beacons. The beacon receivers operated at 5700 megacycles and their transmitters at 5775 megacycles. The TM probes included a 247.3-megacycle telemetry link transmitting beacon current drain to indicate beacon health in the radiation environment. The flare probe contained three banks of flares with four flares in banks one and two,and six in bank number three. The flares were used to measure total refraction by noting the optical position of the probe relative to the radar line-of-sight at several critical locations. Four Speedball probes mounted on their launchers at Johnston Island are shown in Figure 3.2.

An instrumented and guided Nike-Hercules was used for the Tight Rope experiment. Its instrumentation consisted of a C-band beacon operating at the previously noted frequencies and a propagation link operating in the telemetry band at 248.6 megacycles. In addition, tracking experiments were performed using C-band beacons piggy-back on several Project 6.2, 6.7, and 9.1a probes. The complex integrated sensor-recording system which was operational aboard the USAS American Mariner, suggested a number of secondary

measurements. Accordingly, these secondary experiments were performed as outlined in Figure 3.4. The general characteristics of the sensors utilized for these experiments are described below:

3.2.1 Precision Tracking Radars (AN/FPQ-4 modified). The four-horn C-band monopulse precision tracking radars are mounted athwart ship aft on the USAS American Mariner. The vertically polarized port radar was utilized for probe tracking while the horizontally polarized starboard radar was used for clutter mapping. The radars utilized the following parameters:

Frequency	Starboard:		5825 Mc
	Port:	Transmit	5700 Mc
		Receive	5775 Mc
Antenna diameter	16 ft		
Peak-power	3 Mw		
Pulse length	1 μsec		
PRF	285 pps		
Receiver noise figure	5 db		
Receiver bandwidth	2.2 Mc		
Range (one-square-meter target)	310 nautical miles (0 db S/N - single hit)		
Beamwidth	0.8 degree		

The effective direction of arrival of the signal was measured by one four-horn monopulse receiver system of these radars, operated in the amplitude-sensing monopulse mode. The DAMP system utilizes two IF receiver systems paralleled after first detection. One receiver system is also used for tracking purposes and utilizes filtered AGC-controlled receivers. The other receiver system utilizes unfiltered wide dynamic range receivers to obtain maximum bandwidth undistorted information. Signal strength measurements made by both systems are presented. The jitter measurements contained in this report are presented by means of the tracking receiver output signals only. These signals are restricted in bandwidth and somewhat contaminated by AGC action. The uncontaminated wide dynamic range receiver information is available at the DASA Data Center, General Electric TEMPO, Santa Barbara, California.

3.2.2 L-band/UHF Radars. These non-tracking radars share a common 28-foot-diameter antenna and are slaved to the C-band radars or otherwise directed as desired. The direction of arrival of the signal cannot be determined from these radars. The radars utilized the following parameters:

	L-band	UHF
quency	1300 Mc	425 Mc
mwidth	2 degrees	6 degrees
Peak power	2 Mw	2 Mw
Receiver NF	5 db	4 db
PRF	285 pps	285 pps
Pulse length	1.7 μsec	1.7 μsec
Range (1 m^2)	266 nm	204 nautical miles (0 db S/N - single hit)

3.2.3 Telemetry Tracker. This device is a four-lobe interferometer type, passive tracking system with the following characteristics:

Antenna	12 ft square; 4 bowtie-type antennas
Gain	18 db
Frequency	247.3 Mc (Speedball), 248.6 Mc (Nike-Hercules)
Beamwidth	20 degrees
Receiver	-160 dbw

The direction of arrival of the signal can be determined by this device. This information is included in the data discussed in this paper.

3.2.4 Transit System. This system utilizes a stable oscillator (1 part in 10^{10}) designed to precisely measure the doppler content of several stable phase-locked transmissions radiated from a moving vehicle. The system was designed for precise navigation using the Transit satellite and is complete with a digital computer. The system was modified to precisely measure the signal strength and doppler content of the 950-megacycle signal from the 6.1 rockets fired during the Blue Gill and Check Mate events. The direction of arrival of the signal cannot be determined by this omnidirectional device.

3.2.5 Other Facilities. In addition, the USAS American Mariner contains a self-sufficient operational capability including communication and crytographic facilities, digital and analog computers for real-time designation and post-mission data reduction, as well as operational displays and equipment interconnecting switching for radar designation and real time output.

3.3 RESULTS

A total of 110 minutes of precision radar tracking data was obtained by DAMP on 23 probes launched during the five Fish Bowl events. The details of this data and the

numerous and varied other measurements can be found in the other volumes of this POR. It is the intent of this section to summarize the most important obvious effects noted during each test, presented in order of decreasing altitude.

3.3.1 Star Fish Prime. The objectives of this radar tracking experiment were achieved through the launch of six probe rockets (probe No. 2 through probe 7). A seventh rocket (probe No. 1) was tracked to provide trajectory data for Project 9.1a prior to detonation. All probes carried a C-band frequency beacon (5,700 megacycles for interrogation and 5,775 megacycles for reply) for tracking data, and the three 6.13 Speedball probes (probe No. 3, probe No. 4, and probe No. 6) each carried three banks of pyrotechnic flares required for the total refraction measurements.

All beacon systems performed well and provided a clean signal-to-noise margin of at least 45 decibels. Probe No. 2 (6.7/6.13) was not tracked due to shipboard operator error. A brief return was received from this probe. Failure to acquire and track probe No. 2 within the allotted time necessitated the launch of probe No. 3 as a preburst backup.

Very high scintillation or pulse-to-pulse signal strength variations were present during the recovery period. occurring at random intervals, until recovery to the nominal

signal was virtually complete

The modified AN/FPQ-4 tracking system integrates six or more of its non-compressed, non-coherent pulse returns to establish tracking commands. Hence, the radar tracking system saw the four-pulse, H-0 blackout as a small disturbance. In addition, these circuits smooth over large pulse-by-pulse signal variations, and therefore, track was maintained. Some small range and angle jitter errors were present. The angle errors were no larger than two mils, and they were present only during the first second after burst. Although the H-0 effect described above did not cause the radar to loose track, the data obtained illustrates several important parameters for the defense designer to consider. First, the one way beacon-radar link experienced an average of

This would mean [a 40-decibel two-way attenuation of skin signals or a 10:1 reduction in radar skin range] for that period. Secondly, radar systems or ground-space communications systems such as missile guidance relying upon transmission of information would

Finally, this problem would be extended over a large region due to the vast areas intensely ionized by this uncontained burst.

Three additional probes were tracked over the period from H + 1200 to H + 3292 seconds. No additional tracking difficulties were encountered.

At H + 21.6 seconds at 98.5-kilometer altitude, track was abruptly terminated when the beacon was lost within a single pulse also shown in Figure 3.7. This abrupt track termination also occurred on the next probe at H + 944 seconds at 225-kilometer altitude.

To establish the reason for these failures, several probes during the subsequent nuclear tests were instrumented with telemetry monitoring beacon health by means of current draw. A preliminary review of the beacon health data indicates that most beacons performed well until they penetrated the ionized D-layer. After penetration, they are subject to random drop-outs and fail to respond. This failure seems to correlate with short circuit current drain. At this writing,

there seems to be no correlation between this effect and the time-space history of the burst phenomenon such as debris location and associated ionization. Generally, radar track is maintained through this dropout period. On the other hand, during two tracks, severe beacon dropouts occurred prior to burst or below the D-layer. These two beacons also displayed other symptoms such as frequency shift and are considered faulty. On one occasion, track was manually terminated, and a backup probe was launched due to this problem.

As a result of these findings, track termination of the two Star Fish probes is presently attributed to beacon dropout failure in the presence of a nuclear burst environment. However, at present, these effects can not be correlated with bomb phenomenology such as the penetration of dense stratified debris or the like.

No obvious effects were observed during the following four probe tracks.

Figure 3.8 depicts the DAMP geometry during Star Fish Prime from the point of view of the magnetic-zone radar backscatter measurements. By locating the ship 356 kilometers from Johnston Island, the radar line of sight would

be perpendicular to the magnetic field line passing through the burst at the 100-kilometer-altitude point. This region where the field lines through the burst intersects the ionosphere at 100-kilometer altitude will be called the magnetic zone. The maximum backscatter effect from the Beta radiation trapped by the earth's magnetic field was expected at the magnetic zone. Possible interference with the warhead destruct frequency prevented the UHF/L-band radars from observing the actual burst. At burst time (H+0) the C-band radar was scanning the burst region; however, no effects were noted. Twenty seconds after burst, the UHF/L-band radars were also scanning the burst region, also with no measured effects. At H + 75 seconds, all three radars started mapping the magnetic zone using a 5-degree spiral scan. The shaded area in Figure 3.8 shows the region from which the UHF radar obtained measurements. No effects were seen with the L-band and C-band radars.

All three radars continued to scan the magnetic zone and the burst regions alternately at 50-second periods of time; however, no radar returns were observed after H + 115 seconds. At H + 800 seconds, the radars proceeded to map the entire hemisphere. No measured returns were received.

Figure 3.9 is a presentation of the UHF observations from the magnetic zone. This type of data presentation will be used repeatedly in this report. The technique used in generating such a display is as follows. The output from the radar receivers is used to modulate the Z-axis, or the intensity of an oscilloscope. Time from each transmitted pulse, which is proportional to radar range, is used to control the vertical deflection of the oscilloscope. Therefore, for each transmitted pulse from the radar, a single vertical sweep on the face of the oscilloscope is generated. The intensity of the spot produced during this sweep is modulated by radar receiver video amplitude. All targets appear as a bright spot on the vertical sweep. As the oscilloscope face is photographed on continuously moving film, all returns are recorded graphically in the type of display shown. All targets observed by the radar appear as continuous traces. These intensity modulated films are quite useful in determining an overall picture of what the radars received. To obtain detailed information such as target amplitude and width, however, it is necessary to investigate the individual radar returns for each transmitted pulse. The inserts are samples of the UHF returns at various times. From this type

of display, one can obtain both target amplitude and width on a pulse-by-pulse basis.

A Transit satellite was tracked approximately one hour after burst. The doppler data indicates that the satellite transmissions passed through two regions of exceptionally high electron density—at equal distances before and after the closest approach of the satellite to the DAMP ship.

3.3.2 Check Mate. For the Check Mate experiment, the ship was positioned so as to place the radar line-of-sight through the burst parallel to the magnetic field lines at burst time. Burst was intended to be at 191 degrees bearing from Johnston Island at 70-kilometer distance. Actual burst was at 186.8 degrees bearing from Johnston Island at 75.6-kilometer distance.

The fireball, which rapidly expanded

is depicted in its relationship to the ship and the early time DAMP Speedball rocket in Figure 3.10. The northern auroral region due to the debris beta particles is shown as the cross-hatched area projected from

the debris along the geomagnetic field lines into the lower ionosphere.

Three DAMP rockets were scheduled, with a fourth available for backup to the first. Due to rocket payload delivery schedules, only one telemetry payload was available. The firing sequence and payloads were:

H - 70 seconds	Telemetry package + C-band beacon
H + 10 seconds	Backup probe, C-band + lead weights (not fired)
H + 500 seconds	Flare package + C-band beacon
H + 1020 seconds	C-band beacon + leadweights

All three probes were acquired and tracked from expected A-time at three degrees elevation to splash. The backup probe was not required and, therefore, not fired.

A single-pulse, one-way beacon dropout of at least 55 decibels occurred at H-0. Complete recovery and normal track occurred within several pulses. Normal track was maintained until splash. No obvious effects were observed during the remaining two probe tracks. Figure 3.10 indicates that the rise of the disturbed region was more rapid than the rising probe along its trajectory. Thus, the probe never encountered the disturbed region nor did it

encounter the field-aligned ionization emanating from the rising debris. Thus, there was no effect measured at C-band.

The 247-megacycle telemetry (TM) link from this probe to the ship experienced

some of the early excursions may be attributed to operator acquisition difficulties.

The different effects noted from the same source along different propagation paths are probably the result of the geometry of propagation relative to the magnetic field oriented beta-patch. Figure 3.10 shows that the beta particles emanating from the debris remaining in the burst region will

to Johnston Island. Several optical photographs indicate a residue of debris near the initial burst location.

The lack of C-band effects, other than the instantaneous effect, is an indication of the lack of intense immediate X-ray ionization in the D-region. Nevertheless, the

The second probe launched was equipped with the Speedball flare-ejection system. Two flares functioned at approximately H + 570 seconds and were noted to be within the slaving tolerances of the optical system, indicating that no refractive bias greater than could have existed at this time.

Figure 3.13 is a geometrical representation of the C-band, L-band, and UHF radar backscatter measurements. All three radars were designated to the region of burst at H - 0. After burst, the radars followed the rising fireball and at the same time executed a 5-degree spiral scan about the rising fireball. An operator error caused the digitally programmed designation data to be inserted early, and the antennas were pointing high in elevation. However, at H + 13 seconds, the UHF radar observed the rising fireball in its antenna sidelobe. The insert on Figure 3.13 shows the amplitude and width of a typical fireball return during this period.

At H + 120 seconds all three radars were designated to the magnetic zone (shaded area, Figure 3.13). No returns were seen at C or L-band frequencies; however, backscatter data was obtained by the UHF radar. Figure 3.14 shows the actual scan pattern used and the limit above which no UHF returns were seen. The second scan through the same region which occurred 50 seconds later showed only brief UHF returns at H + 202 seconds. The inserts show the amplitude and width of the returns at various times.

From H + 250 seconds until H + 350 seconds the burst region was scanned, again with no measured returns. After H + 350 seconds the entire hemisphere was mapped, with no measured effects.

3.3.3 King Fish. For this test the ship was located 95 kilometers magnetic north of Johnston Island (11 degrees true bearing) and along the magnetic field line through burst. The King Fish burst occurred at

or near the normal maximum free-electron level of the region. The burst produced a rapidly expanding fireball. The fireball rose rapidly, elongating vertically as it rose. The shape of the disturbed region in relationship to the project 6.13 probes is shown in Figure 3.15.

The rising fireball was accompanied by a strong field-aligned auroral region emanating from the bottom of the fireball. This auroral region remained trapped in a relatively concentrated tube aligned along the field lines through the burst region, although the fireball and the debris contained within it rapidly rose above the burst region. This anomalous effect continued until

when the magnetic field snapped

back to its original position, and the narrow auroral tube expanded to cover the very large debris area dissipating its intensity.

For the King Fish event, seven rockets equipped with C-band beacons were scheduled to be tracked; four DAMP Speedballs, and three Project 6.2 rockets. Firing times and payloads of probes for this operation were (all probes carried C-band beacons):-

1	H - 350:	DAMP telemetry, 82 degrees
Backup	H - 270:	DAMP backup to No. 1, flare probe 78 degrees firing elevation
2	H - 120:	Project 6.2, Honest John-Nike-Nike (Tracker No. 2)
3	H + 200:	DAMP telemetry
4	H + 780:	Project 6.2, HJ-N-N
5	H + 1010:	DAMP telemetry
6	H + 1500:	Project 6.2, HJ-N-N
7	H + 1960:	DAMP backup

The H - 350-second probe and H - 270-second backup to this probe differed in launch elevation by 4 degrees. The trajectory difference was designed to compensate for the firing time difference and permit both the main probe and

the backup to be behind the burst area at burst time along line-of-sight parallel to the geomagnetic field lines. A flare backup telemetry probe would be competing with the first telemetry probe at the same look angle and frequency.

The H - 350-second probe was acquired normally, but the radar track became intermittent after the backup rocket firing time.

the probe was tracked through burst.

A single-pulse, one-way beacon drop

probe-to-ship radar link was experienced at H - 0. Return to the pre-burst signal strength occurred within several pulses. However, the returns were

Angle tracking was noisy during this track period. Figure 3.15 indicates that the fireball rose through the line-of-sight defined by the ship's radar and the probe

This probe carried a telemetry link operating at 247.3 megacycles. The link was monitored both on the ship and from the launcher area on Johnston Island. Figure 3.16 shows that blackout of this signal was experienced at

Johnston Island

The Johnston station utilized a single-helix antenna and low-sensitivity receiver specifically for pre-launch monitoring, which explains the very low signal margin with which the data was obtained. At seconds the signal recovered. The beacon health sub-carrier signal indicates 0 pulse recurring frequency (PRF) or that the beacon was not triggered from H + 10.5 seconds through H + 14.4 seconds. From H + 14.4 seconds through the remainder of the probe flight, the beacon was pulsed at 285 PRF. Occasional periods of noisy information occur, probably as a result of the low signal being fed to the telemetry discriminator. In addition, the usual dropouts are seen.

From the ship, C-band beacon

Between

During the period from

The track during this period was accompanied by some angular jitter, and severe beacon dropouts lasting 0.1 second or more were encountered on some occasions. Track was maintained until splash at H + 101 seconds. During this period, the severe dropouts continued. These dropouts correlate well with the telemetry data.

The above effects again indicate the localized nature of debris and beta-absorption.

The Project 6.2 rocket scheduled for launch at H - 120 seconds was not tracked. It had been intended that the other C-band radar (Port radar) track this probe to determine trajectory until H - 30 seconds. However, the analog designation computer had to remain programmed through the H - 350-second Speedball trajectory, since this rocket was experiencing intermittent track at this time. Designation data was, therefore, not available for the other radar, and the 6.2 rocket was not acquired. The sixth rocket, also a Project 6.2 probe, was triggered for several hits, but no solid target was seen, and the rocket was not acquired. This is presumed to be due to a faulty beacon.

Four rockets were tracked through the disturbed region after the H - 350-second rocket track. The trajectory of the third probe, tracked from H + 212 through H + 533 seconds is shown in Figure 3.15. No difficulties, other than an occasional brief beacon dropout as described above, were encountered on these probes.

A flare-carrying probe originally scheduled to be fired as backup at H - 220 seconds was fired at H + 1960 seconds. Track was normal. Three flares were recorded. A maximum track deviation of 3.4 mils was measured. This deviation was within the normal pedestal slaving tolerance, and the data indicated no major refraction at that late time.

Due to what is believed to be equipment failure, the telemetry tracker was unable to automatically track any of the 6.13 telemetry Speedballs. Therefore, no 247-megacycle absorption was measured, and no angle jitter measurements are available at this frequency for King Fish.

The opacity and spatial coverage of the fireball at C-band is obvious from the results of this experiment.

The angular regions examined by the UHF, L-, and C-band backscatter measuring radars are depicted in Figure 3.17. All three radars were pointing at burst at H - 0. The warhead was visible at UHF/L-band frequencies prior to H-0 time as shown in Figure 3.18. At burst, all radar returns completely vanished from the 6-degree UHF radar beam for

At L-band, this absorption, as might be expected, was for a shorter

The L-band beam is approximately 2 degrees wide. However, and this substantiates the trend, at the 1-degree beam C-band the burst was

The video records from the three radars also show distinctly increased noise background at

H - 0 time, and at the C-band frequency this increased noise is coincident with the blooming fireball target. The inserts in Figure 3.18 show the amplitude and width of the radar returns at the various times.

It was intended that the radars would commence scanning the fireball at H - 0, while following the rising fireball in elevation for 60 seconds thereafter. The gradual rise in elevation was not inserted into the digital computer programming the radars due to human error. Also, the scan of the magnetic zone (cross-hatched region of Figure 3.17) was begun late at H + 300 seconds, explaining the lack of observed auroral backscatter returns. Again, no reflections were observed during the complete hemispheric mapping.

It is, however, significant to note that while UHF energy was

(See Figure 3.18.)

3.3.4 Blue Gill Triple Prime. For this test the ship was positioned so that tracking radar No. 1 (Port radar), while tracking the first Project 6.13 probe, would be looking parallel to the magnetic field lines through the fireball

debris at the time the fireball was expected to rise into the D-layer. This placed the ship 106 kilometers from Johnston Island on a bearing of 11 degrees. Actual burst occurred 36.41 kilometers from Johnston Island on a bearing of 192.79 degrees Five probes were scheduled, with a sixth available as backup for the first DAMP probe. Two Project 6.2 rockets were to be tracked. The firing schedule was:

1 H - 312: Main probe; flare package + C-band beacon

2 H - 180: Backup to 1; flares + C-band beacon

3 H + 180: Flares + C-band beacon

4 H + 900: C-band beacon only; Project 6.2, Honest John-Nike-Nike

5 H + 1320: Flares + C-band beacon

6 H + 1860: Project 6.2, Honest John-Nike-Nike (C-band beacon only).

All DAMP rockets were to be fired at 190 degrees true and 82 degrees firing elevation. Project 6.2 rockets were north, fired between 10 degrees and 20 degrees. If the backup rocket was not used at H - 180 seconds, it was not to be fired at a later time. Acquisition was successful on all probes, and most were triggered on the launcher.

The first two probe tracks after burst are shown in Figure 3.19. A signal strength record of 950 megacycles was obtained for the H-160, 6.1 probe. The nominal, not actual, trajectory of this probe is also shown on this figure for correlation purposes.

The first probe was acquired about three degrees elevation over the launcher. Track was well-behaved until approximately 40 degrees elevation, at which time track became oscillatory, beacon faded, and track was lost at 70 seconds after lift-off, during a deep fade.

The backup probe was, therefore, fired at H-180 seconds. Solid track was established around three degrees elevation and continued through burst.

At burst, the backup probe was near apogee. The propagation path was some 30 degrees above the burst in the plane of the magnetic field through burst. The one-way beacon signal experienced

This effect was similar to that experienced during Star Fish Prime and is shown in Figure 3.20.

Track was maintained through this period, although some angle and range jitter was experienced. No serious effects were noted

until track was lost due to the target jumping out of the range gate at H + 55 seconds. Shortly thereafter, the target was completely lost and never reacquired, although the radar pointing measurements indicate that the radar was directed to the vicinity of the target for a reasonable period after loss of track. At this writing, there appears to be no correlation between the propagation paths and the fireball or debris locations.

The next probe, launched at H + 180 seconds was acquired at H + 190 seconds. Several important effects were noted during this track. These effects correlate with the rise and expansion which occurred as depicted in Figure 3.21. These debris rise and expansion rates are based on the limited optical information available to date. Specifically, the initial rise and expansion rates were obtained from Reference 3.

The late-time (after two minutes) debris rise and expansion history of the debris was obtained by triangulation of the all-sky-camera photographs taken on the DAMP ship and on Johnston Island. The cameras were calibrated and read at SRI. The triangulation and plots were performed in accordance with this information. Due to residual ships-motion effects on the time exposure photographs, as well as uncertainties in camera calibration, absolute camera alignment and the non-uniform nature of the debris toroid angular errors up to 2 degrees can occur. This error amounts to uncertainties in the order of $\pm$10 kilometers in the determination of the debris locations.

During the period from H + 240 seconds to H + 300 seconds, the propagation path from the probe to the radar traversed the region through the near arm of the debris toroid. At that time, a period of angular and range jitter was experienced. This effect was not intense. However, during the period from

as shown on Figure 3.22 was encountered. During this period, a deep probe antenna lobing null was encountered and track was lost. Upon reacquisition, the propagation path again passed through the center of the toroid without encountering the actual debris regions. The tracking signals were not grossly affected during this period.

During the period from H + 480 seconds and H + 487 seconds, the propagation path again crossed the near arm of the debris toroid. This time, a very small attenuation accompanied by some angle and range jitter was experienced. Track was maintained although occasional beacon dropouts were encountered.

At H + 546 seconds, track was terminated due to an abrupt cessation of the beacon signals as the propagation path approached the far arm of the toroid. Additional study will be required to establish if this effect was due to a beacon dropout or propagation absorption. A total of three additional probes were then tracked. No effects were noted other than occasional beacon dropouts.

At burst, the Transit tracking system at 950 megacycles was tracking the doppler signal of the 6.1 probe launched at H - 190 seconds. The signal strength record at H-0

indicated

The data from this test indicate several important factors, namely:

1. The lessons learned during the initial Star Fish Prime tracking periods were repeated during this much lower altitude, lower yield burst.
2.

Six flares were observed during Blue Gill Triple Prime, including a pre-burst flare at H - 242 seconds. The pre-burst flare was offset 1 milliradian in azimuth and 3/4 milliradian in elevation. The flares observed after burst were all measured to be within 1-1/4 milliradians in elevation and 1 milliradian in azimuth with respect to the C-band tracker axis.

The areas of interest from the radar backscatter viewpoint are shown in Figure 3.23. Because of possible UHF telemetry interference, the UHF/L-band radars were not permitted to illuminate the burst point; they were slaved to the C-band radar 20 seconds after detonation.

The C-band radar again recorded return signals at detonation and for approximately 2 seconds thereafter. The test plan called for a programmed rise in antenna elevation to observe the rising fireball. This was accomplished, with UHF/L-band illumination after H + 20 seconds, with no measurable effects. Later however, at H + 26 seconds, a return was recorded by the L-band radar

and as would be expected, the UHF radar observed definite returns still later at H + 38 seconds. These returns are shown in Figure 3.24 as an intensity-modulated display. Figure 3.25 shows the amplitude and width of the return pulses at various times after burst.

All three radars continued to see target returns while scanning the fireball region up to maximum fireball height at 70 kilometers. The elevation of the radar antennas was increased to scan the broad region above the fireball; however, no measurable targets were recorded up to an altitude of 210 kilometers.

The radars returned to burst altitude at H + 320 seconds, passing rapidly down through the fireball region (so swiftly that sustained targets would not have been observed). Both the L-band and UHF radars received

substantial signal returns in the burst region where detonation had taken place some 350 to 500 seconds before. No positive C-band returns have yet been identified in this data, yet the background noise rose substantially exactly as it did on this and other tests when reflecting targets were present.

The radars were slewed to the magnetic zone at H + 550 seconds where large-area scanning was continued for approximately 100 seconds. No target returns were visible in the measured data.

Finally, broad hemispheric mapping was conducted with negative results.

3.3.5 Tight Rope. The Project 6.13 primary objective on Tight Rope was to track an accurately placed Nike-Hercules probe behind the fireball for extended periods to determine C-band absorption and any other effects which might occur while tracking through the Tight Rope fireball. For this reason, the ship and the Nike-Hercules probe trajectory were accurately positioned so that the probe would be along the line-of-sight from the ship to the burst point, that is, behind burst point at H-time, and remain behind the

rising fireball for several tens of seconds. The optimum ship position was 10 kilometers magnetic north of the launcher.

The Project 6.13 Nike-Hercules probe was scheduled to lift off 5 seconds earlier than the Tight Rope Nike-Hercules. Burst of the live round was to occur

after lift-off at a position of

3 kilometers south of the launcher. Burst actually occurred at 3.35 kilometers south of the launcher while the instrumented probe and the ship were located precisely as desired.

The burst produced a small slowly rising fireball which shortly developed into a well-defined toroid. The geometry of the toroid with respect to the probe trajectory, and ship location is shown on Figure 3.26.

At H-0 both the one-way beacon and two-way skin return experienced a single-pulse complete blackout in the order of /N as shown on Figure 3.27. Upon recovery, the skin

over pre-blackout values. The double path length for the skin return resulted in double attenuation.

In both cases, the signal returned to normal within 2 seconds.

A normal track, almost devoid of angle or range error, was maintained as shown on Figure 3.26 until H + 36 seconds when the propagation path crossed the rising near arm of the toroid. At this time the one-way beacon signal experienced

as shown in Figure 3.28. The attenuation was accompanied by large range and angle error fluctuations. Track was maintained through this region. At the same time, the skin return was

as shown on Figure 3.29.

After passing from behind the near arm of the toroid, normal track was regained. In fact, a careful investigation revealed no detriment in tracking performance although the propagation path went directly through the center of the relatively small toroid.

As the propagation path crossed the far arm of the toroid, an effect similar to the above but of far less magnitude was experienced by the C-band track. The difference in the severity of the transmission effects as the

propagation path swept over the near and far arms of the toroid can be due to either the time lapse of 25 seconds, permitting dissipation of the disturbance, or the non-homogenious nature of the disturbance in the toroid, or both. Late-time photographs show a spotty appearance of the toroid indicating non-homogeneity in electron concentration. No additional C-band problems were encountered for the remainder of the track. No beacon dropouts occurred after the one-pulse blackout at H-0.

A propagation link operating at 248.6 megacycles was maintained between the instrumented probe and the DAMP ship. Several receivers were also available on Johnston Island. No information other than propagation signal strength was carried over this link. The signal strength as received by the shipboard telemetry tracker is contained in Figure 3.28. In addition, the servo error signals to the tracking mount are shown.

This link

Complete blackout again occurred as the propagation path swept across both arms of the toroid. As in the C-band tracker

case, the signal returned to normal as propagation passed through the center of the toroid. A further effect was noted as the propagation path swept across the original burst region, from H + 89 seconds to H + 105 seconds. This effect was not as severe and transmission was possible. This transmission was accompanied by very large angle error fluctuations.

The telemetry receivers on Johnston Island recorded a blackout and recovery period similar to that described above. However, full recovery had not been achieved at [redacted] when the recordings were inadvertently terminated. As was observed from the measurements of the Blue Gill Triple Prime experiments, the initial non-field-aligned ionization from this small yield causes important attenuation which must be considered for tactical purposes. Further, the rising, expanding but concentrated, debris causes long-lasting but precisely defined areas of attenuation and/or blackout. Thus, long-lasting, self-blackout conditions, occurring as a result of intercept detonations, are a definite problem.

Radar backscatter measurements for the Tight Rope event were combined to measuring the radar returns at UHF, L-, and

C-bands of the fireball and the instrumented Nike-Hercules through behind the fireball. It was hoped that the Starboard C-band tracking radar would skin track the instrumented Nike-Hercules with the UHF and L-band radar slaved, while the Port radar would beacon track.

Due to an operational error in radar and slave pedestal assignments, the reflections from the fireball and the Nike-Hercules were obtained only between H + 44 and H + 54 seconds. However, since the burst was some 4 kilometers lower than nominal, the period H + 44 to H +54 seconds coincide with the period during which the debris, the ship, and the instrumented Nike were colinear.

Figure 3.30 shows the fireball and rocket returns on all three frequencies. The C-band beacon tracking radar experienced attenuation and backscatter from H + 30 seconds to H + 40 seconds. During the times shown, the Nike-Hercules was behind the toroidal debris, and while the beacon returns are visible, indicating transmission through the debris area, reflection from the debris is present also.

3.4 CONCLUSIONS

Several important conclusions concerning tracking radars and other systems can be drawn from the results of the 6.13 measurements. The initial radiation pulse for each of the events produced

over the propagation paths of the experiments. The propagation medium during recovery following the initial black-out appears to be very nonhomogeneous, leading to

The attenuation, in general, dissipates prior to the cessation of the pulse-to-pulse noise. The severity of this attenuation and the length and type of black-out has been seen to vary considerably with altitude and yield and the propagation geometry.

The DAMP Fish Bowl measurements show that transionospheric propagation through the disturbed region for frequencies can be adversely affected

for longer than after the burst for detonations within the sensible atmosphere. On the other hand, these measurements show that the disturbed region is sharply defined to RF propagation.

measurements are not available for propagation through the disturbed region produced by bursts occurring above King Fish. However, lower frequency measurements indicate that propagation through these regions at will be affected.

Active pulsed radar backscatter returns were seen from the UHF/L-band and C-band radars from the fireball or debris region and from the auroral-type clutter region to the north. These returns were observed to extend up to tens of kiloyards in range, fluctuating in amplitude at any given range in a random fashion.

With regard to the frequency and time behavior of these returns, the following trends were observed:

1.

2.

Page 72 deleted.

On the other hand, systems relying upon the pulse-by-pulse or statistical information from the received radar signal as well as transmission of information by ground-space communication links, such as missile guidance or satellite measurement devices, will be adversely affected. These effects could [redacted] Further, the effect will not be localized.

These initial effects will also be present for bursts within the sensible atmosphere. However, the effects will not cover as large a region. In general, the region will shrink with the burst altitude and yield. In addition, long-time blackout and tracking difficulties severe enough to cause loss of track and complete loss of transmitted information will occur for propagation paths passing through the disturbed region produced by the detonation. This effect can persist in the [redacted]. The effect is very localized and, as such, may be circumvented by multiple emplacements or other similar schemes.

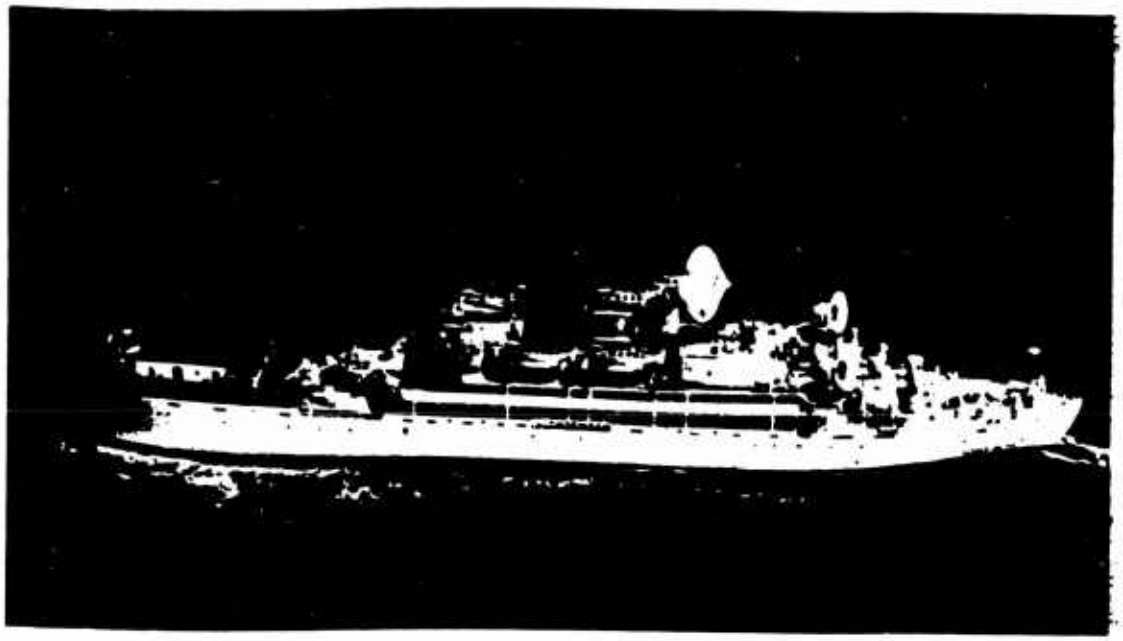

Figure 3.1 USAS American Mariner. (AMC photo)

Figure 3.2 Speedball probes, Project 6.13. (AMC photo)

	ALT (KM)	YIELD	SHIP FROM GRD ZERO (KM)	DATE	PRIME OBJECTIVE	PROBES		
						TM	FLARE	TOTAL
STAR FISH	400	1.3 MT	399.4	9 JULY	JITTER		3	7
CHECK MATE			277.4	20 OCT	JITTER	1	1	3
KING FISH			175.7	1 NOV	JITTER	2		6
BLUE GILL			143.9	26 OCT	JITTER		4	6
TIGHTROPE			13.6	4 NOV	ABSORPTION	1		1

Figure 3.3 Experiment plan, Project 6.13.

OBJECTIVE	SENSOR-FREQUENCY (MC)										
	RIOMETERS			TM	TRANSIT			RADIO METER	RADARS		
	30	60	120	247	150	400	950	440	430	1300	5775
TRACKING JITTER				X					X	X	X
REFRACTION									X	X	X
ABSORPTION	X	X	X	X			X		X	X	X
CLUTTER									X	X	X
6.1 DOPPLER							X				
ELECTRON LINE DENSITY					X	X					
BACKGROUND NOISE	X	X	X					X	X	X	X
DEBRIS SPREAD	X	X	X								
PROBE TRAJECTORY				X							X
EQUIPMENT RELIABILITY								X	X	X	X

Figure 3.4 DAMP ship sensors, Project 6.13.

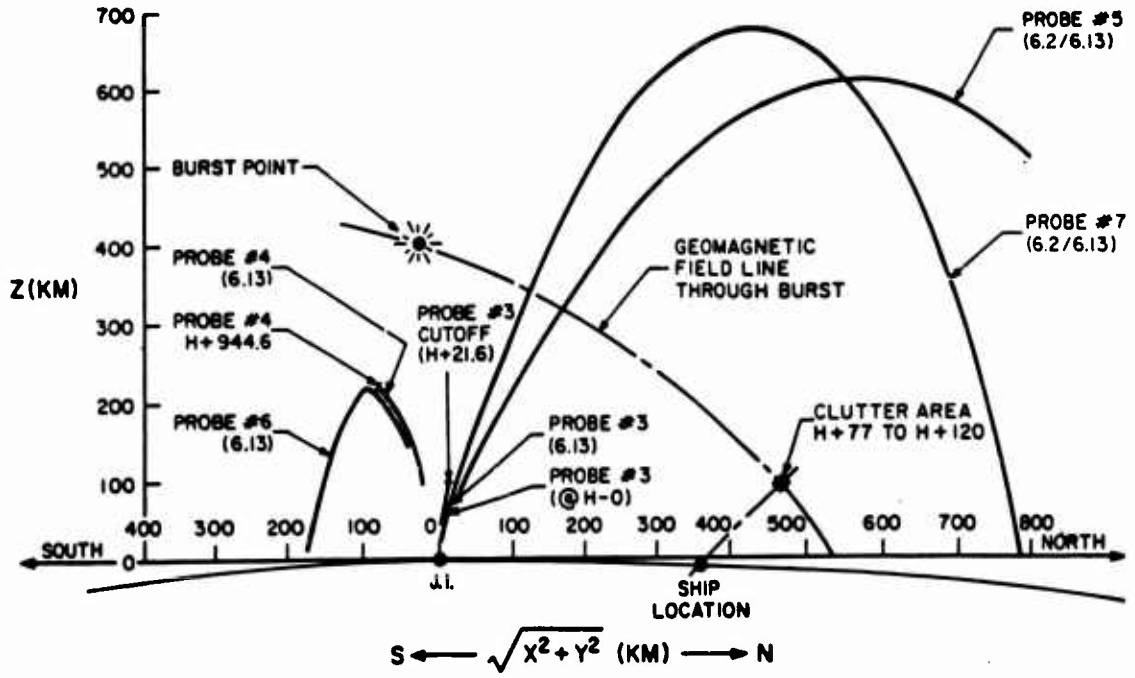

Figure 3.5 Project 6.13 probe trajectories for Star Fish Prime.

Figure 3.6 Star Fish Prime pulse/pulse beacon signal.

Figure 3.7 Star Fish Prime pulse-by-pulse beacon signal, Probe 3.

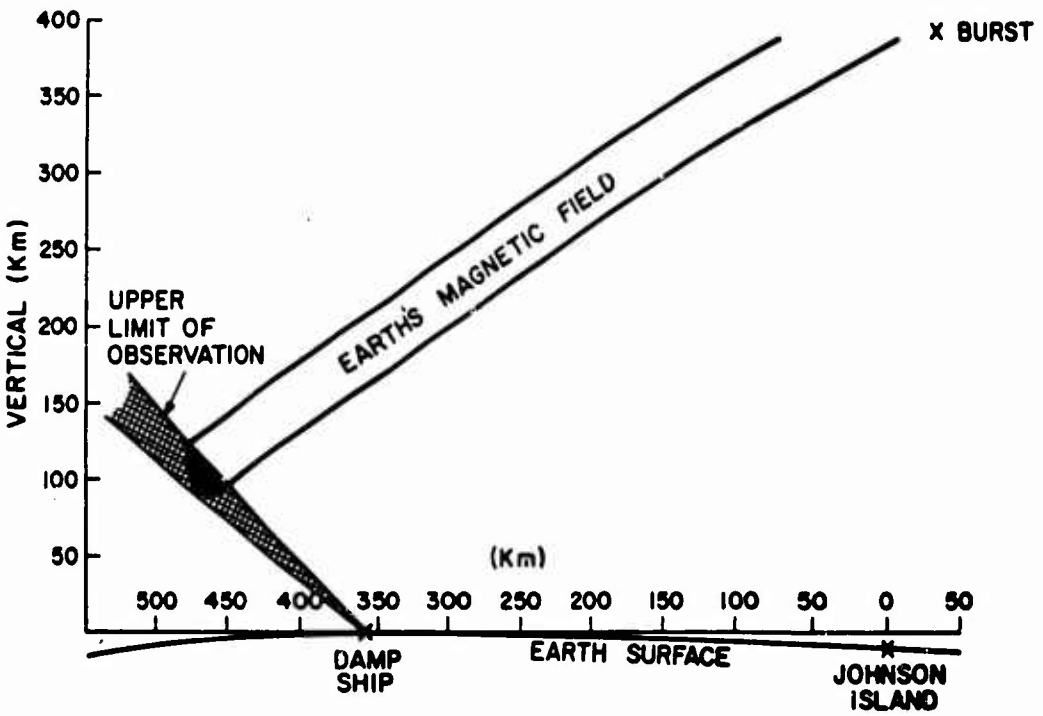

Figure 3.8 Star Fish Prime geometry.

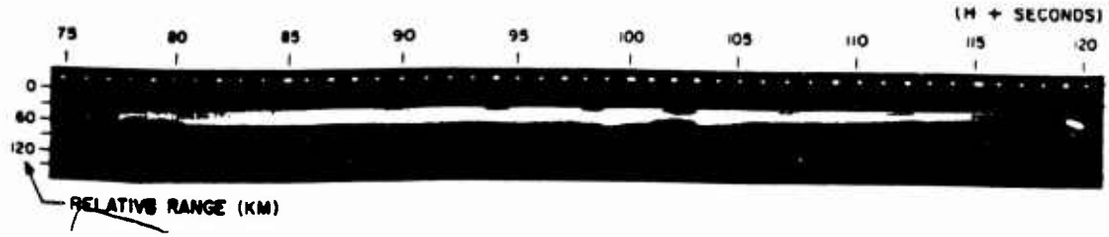

Figure 3.9 Star Fish Prime UHF mapping.

Figure 3.10 Check Mate tracing geometry.

Figure 3.11 Check Mate TM signature, Probe 1.

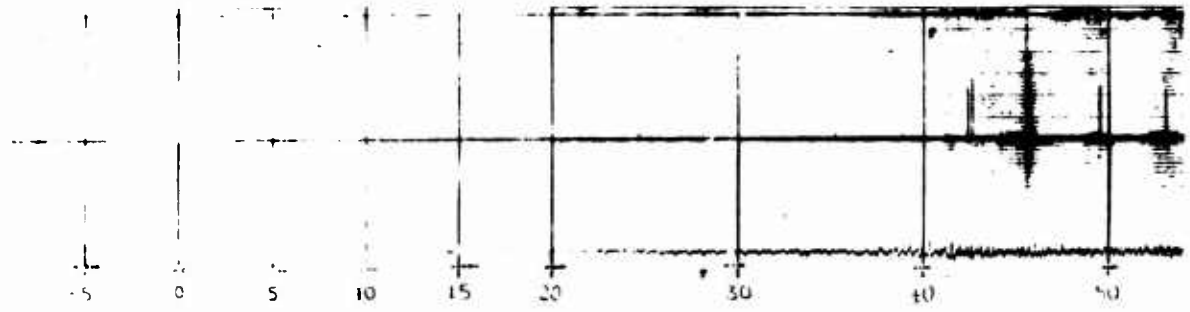

Figure 3.12 Check Mate telemetry record, Johnston Island.

Pages 80, 81, 82 deleted

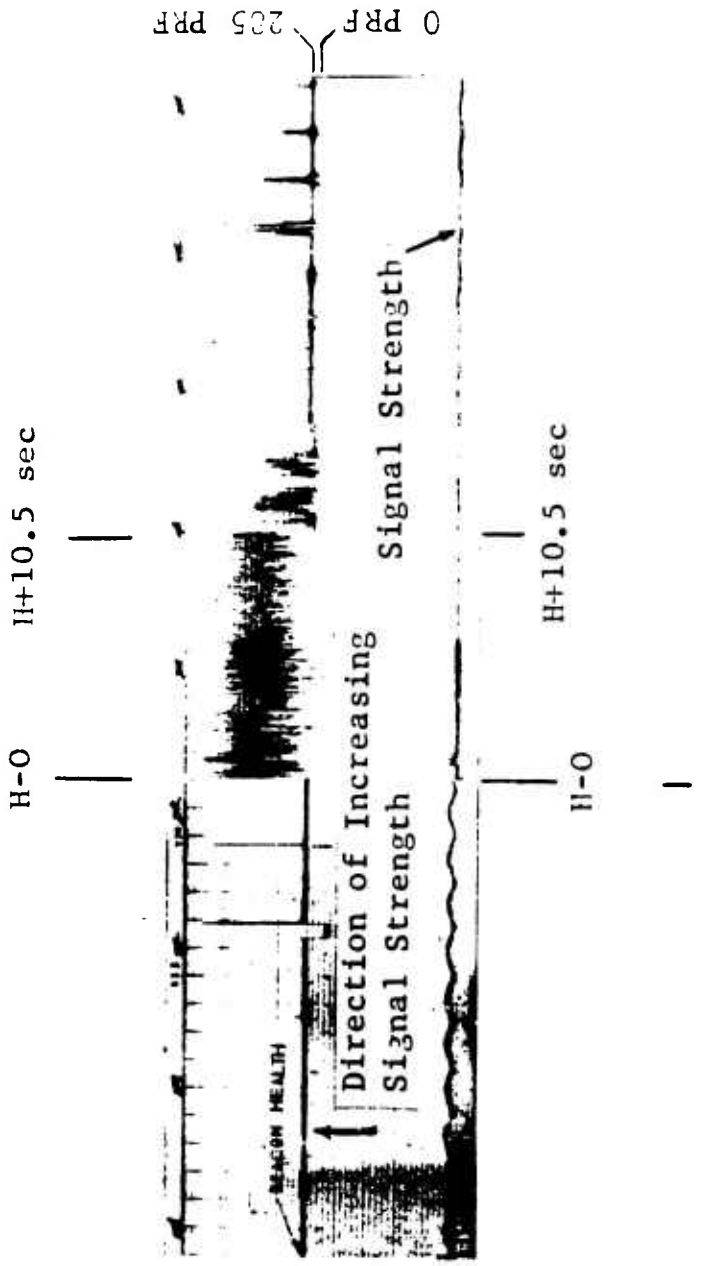

Figure 3.16 King Fish telemetry record, Johnston Island.

Pages 84, 85, 86 deleted.

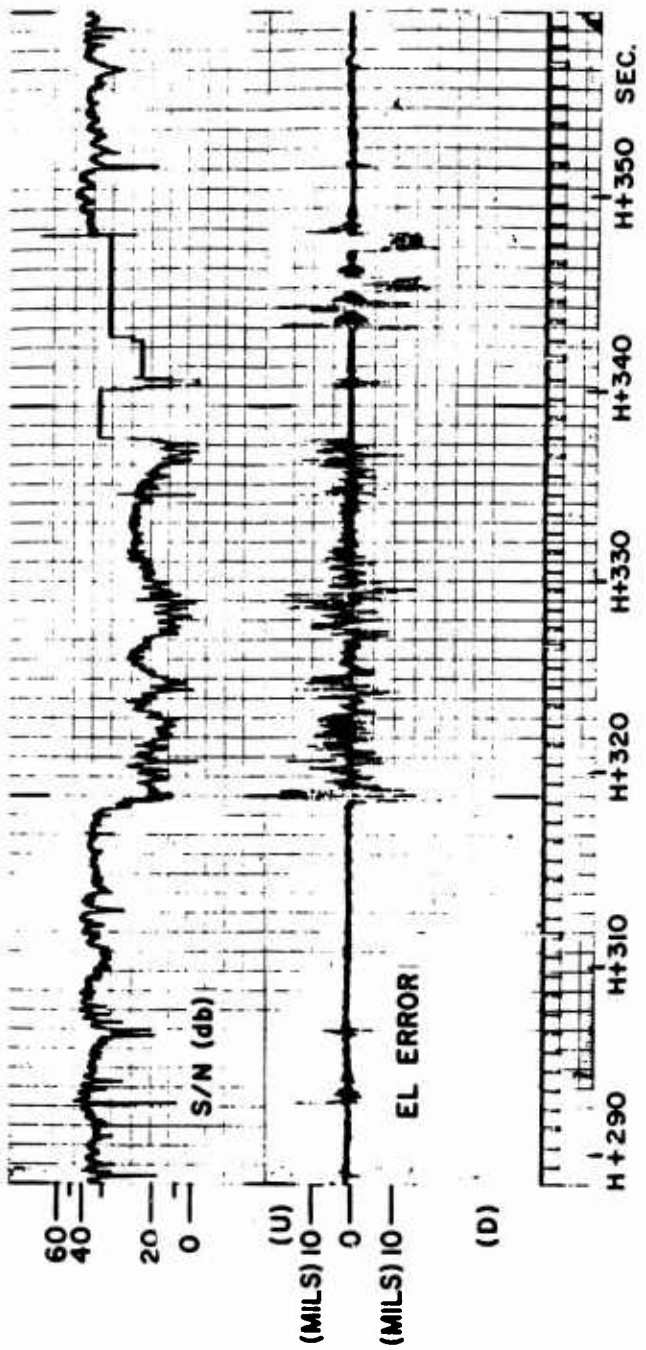

Figure 3.22 Blue Gill Triple Prime tracking anomaly, Probe 2.

Pages 88, 89, 90, 91 deleted.

PART 2

OPTICAL MEASUREMENTS (U)

J. E. Hagefstration, Project Officer

Contributors:

A. F. Wiebe
H. W. Yates
W. Planet

Barnes Engineering Company
30 Commerce Road
Stamford, Connecticut

PART 2

OPTICAL MEASUREMENTS

CHAPTER 4

INTRODUCTION

4.1 OBJECTIVES

The optical measurements made of the high and low-altitude nuclear bursts during the Fish Bowl series were designed to document burst contributions to: (1) damage to direct-viewing optical systems, and (2) saturation and/or blanking of the optical instrumentation viewing the burst proximity. The optical measurements consisted of two parts: (1) viewing the burst directly with visible and infrared detectors, and (2) thorough and systematic visible and infrared measurements of the long-term radiations resulting from the burst proper, weapon debris, and aurora.

4.2 BACKGROUND

Up to the present time the DAMP optical measurements program has included: (1) studies of the radiation characteristics of ballistic missile components (including reentry vehicles, boosters, fragments, and decoys), (2) the nature of the background against which the target must be viewed (including daylight sky, clouds, and stars), and (3) the capabilities of optical systems which are realizable with

state-of-the-art detectors and other components. One background feature which has not been extensively investigated with regard to its influence on the performance of a ballistic missile defense system is the one that accompanies a nuclear detonation. It is imperative to know the influence of both high-altitude and low-altitude nuclear burst environments on optical detection and discrimination systems applicable to ballistic missile defense.

Measurements to test the survival capability of optical instrumentation sensitivities are necessary to determine the design criteria of terminal and other defense systems.

Radiation measurements of the post nuclear burst environmental effects are necessary for that portion of the electromagnetic spectrum from the infrared through the visible and into the ultraviolet to evaluate the phenomena which may be encountered by an optical detection system.

4.3 THEORY

The electromagnetic radiation associated with the nuclear burst that was significant in these studies included the intense, short-time thermal X-ray excited radiation associated with the nuclear reaction itself and the less-intense, long-time radiation associated with the artificial aurora and the debris decay-product cloud. Preliminary

technical information is available, primarily resulting from the Teak and Orange detonations, but the extent of the coverages of the data from the tests do not extend beyond a few seconds after detonation. The Star Fish Prime test was expected to yield data on the background created by the artificial aurora at the extremely high altitude where the typical fireball associated with atmospheric burst was not expected to be present. Information of long-term radiation levels is greatly lacking. The Project DAMP optical studies of the Fish Bowl tests were designed primarily to furnish these data.

CHAPTER 5

PROCEDURE

5.1 TEST PARTICIPATION

The DAMP ship, USAS American Mariner, participated in four tests during Fish Bowl. The important parameters of the tests are listed in Table 5.1. It is informative to note that they can conveniently be divided into high-altitude tests [ ] and low-altitude tests [ ] Additionally, high- and low-yield devices were detonated at both altitudes, further contributing to data cross correlation. A side view of the burst and ship positions for all tests except Star Fish is shown in Figure 5.1.

5.2 INSTRUMENTATION

As a result of experience obtained during each test, the instrumentation was under constant modification during the series. Table 5.2 lists all of the instruments utilized during the tests, and Figure 5.2 shows the instrumentation layout on the DAMP ship.

Instrumentation was divided into three major groups according to usage: (1) burst measurement equipment, (2) long-term (mapping) measurement equipment, and (3) support equipment.

Excessively high radiation levels were anticipated during the initial seconds after detonation, and it was necessary to protect the sensitive electronic equipment (photometers and radiometer) from damage. As they were all positioned on Pedestal 1, the pedestal was directed away to nearly a right angle (in azimuth) from the predicted burst co-ordinates and was trained on the burst only when the levels had decayed sufficiently. The additional burst measurement equipment was under control of the TV-monitored optical director. As a consequence of the protection precautions, it was not possible to view early burst events with the photometers or radiometers. Individual instruments in each of the three major divisions are listed below.

5.2.1 Burst Measurement Equipment. This equipment consisted of the following instruments: (1) total-thermal-power-time radiometer; (2) 70mm high-resolution camera; (3) 16mm DBM-5 cameras; (4) 70mm streak objective spectrograph;

and (5) 35mm Flight Research camera (XR emulsion).

5.2.2 Long-Term Measurement Equipment. The equipment, operated during mapping periods, consisted of the following instrumentation: (1) thermograph and complementary K-24 Star camera (used only on Check Mate and Blue Gill Triple Prime); (2) two 35mm Flight Research boresight cameras; (3) four-channel photometer; (4) R4K1 PbS radiometer; (5) R4K1 thermistor radiometer; (6) all-sky camera operated for Stanford Research Institute (SRI).

5.2.3 Support Equipment. The following equipment supported the gathering of optical flare data from the 6.13 Speedball probes: (1) eight K-19 ballistic cameras located on Johnston Island, and (2) K-24 ballistic (probe) camera operated aboard the DAMP ship.

Another instrument that was utilized as support equipment throughout the entire experiment was the modified Kintel acquisition television system. This system, in conjunction with Optical Director No. 2, was designed to provide pointing information to the slave pedestal carrying instruments committed to the burst phase of the experiments.

5.3 CALIBRATION

Premission background measurements were recorded by H - 60 minutes. All quantitative measurement instruments

were calibrated using as a source of radiation either a standard blackbody (up to 1000°K) or National Bureau of Standards (NBS) calibrated tungsten ribbon lamp. The full dynamic ranges of the instrument outputs (film density or voltage) were covered in the calibration. Also, preburst background mappings were completed to aid in data analysis.

TABLE 5.1 TEST PARAMETERS

Test	Date 1962	Yield	Altitude	H - 0	Slant Range	Elevation	Remarks
	ZULU	kt	km	GMT	km		
Star Fish Prime	9 Jul	1.4 (Mt)	400	09:00:09	560 (Pred.)	44.4° (Pred.)	Obscured by clouds.
Check Mate	20 Oct			08:30:00			Partially obscured by clouds.
Blue Gill Triple Prime	26 Oct			09:59:48			Detonated behind cloud but rose above. Excellent coverage.
King Fish	1 Nov			12:10:06			Excellent coverage. Clouds formed at H + 15 minutes.
Tight Rope	4 Nov			07:30:00			Low altitude, close range.

TABLE 5.2 FISH BOWL INSTRUMENTATION

Instrument	Field of View	Spectral Sensitivity	Emulsion/ Detector	Chop or Frame Rate	Exposure Time	Remarks
35mm Camera						
No. 1	7° x 9°	.38 - .65μ	Super Hypan	12/sec	1/36 sec	Optical Director Boresight
No. 2	7° x 9°	.38 - .65μ	Super Hypan	12/sec	1/36 sec	Pedestal 1 Boresight
No. 3	13.7° x 18.2°	.38 - .65μ	XR (Wyckoff)	32/sec	1/320 sec	Pedestal 2 Boresight. Triple Layer Emulsion
70mm Camera						
High Resolution	3.2° x 3.2°	.38 - .65μ	Tri-X Pan	32/sec	1/720 sec	
Streak Spectro-graph	11° x 12°	.38 - .70μ	Plus-X Aerecon	144 in/sec	N/A	
Long Focus	5.4° x 12°	.38 - .65μ	Tri-X Pan	30/sec	1/1020 sec	Used only on Tight Rope
Long Focus (Spectral)	5.4° x 12°	.38 - .9μ	Infrared	15/sec	1/1020 sec	Used only on King Fish
16mm Camera	10.7° x 8.3°	.38 - .65μ	Tri-X Pan	400/sec	1/4000 sec	High Speed Record of Tests

TABLE 5.2 (CONTINUED)

Instrument	Field of View	Spectral Sensitivity	Emulsion/ Detector	Chop or Frame Rate	Exposure Time	Remarks
Ballistic Cameras						
K-24 (Star)	40° x 40°	.38 - .70μ	Tri-X Aerecon	Sequenced	10, 30 sec	To obtain star background for thermograph
K-24 (Probe)	40° x 40°	.48 - .53μ	Tri-X Aerecon	Sequenced	45 sec	To obtain speedball flare positions
K-24 (Spectral)	40° x 40°	.38 - .70μ	Tri-X Aerecon	Sequenced		Used on Blue Gill Triple Prime and King Fish
K-19 (Probe) (4)	37° x 45°	.48 - .53μ	103-F	Plate	Variable	Positioned on Johnston Island. Probe-flare data
All-Sky Camera	160°	.38 - .65μ	Royal-X Pan	53 sec	53 sec	Stanford Research Institute received data
Photometer						
1	1° circular	4036 Å	6810 PMT	1/50 sec resolution	N/A	Photometers used on all tests. Filters chosen to record selected nitrogen aurora radiation. Nominal half bandwidths of 100 Å
2	1° circular	7000 Å	7102 PMT	1/50 sec resolution	N/A	
3	1° circular	8826 Å	6217 PMT	1/50 sec resolution		
4	1° circular	3892 Å	6903 PMT	1/50 sec resolution		

TABLE 5.2 (CONTINUED)

Instrument	Field of View	Spectral Sensitivity	Emulsion/ Detector	Chop or Frame Rate	Exposure Time	Remarks
Radiometer						
1	2° x 2°	1.8 - 2.8μ	Lead Sulphide	1/50 sec resolution	N/A	Total chop mode
2	2° x 2°	1.8 - 15μ	Thermistor	1/50 sec resolution	N/A	Did not record data
Total Thermal Radiometer	~ 35°	.3 - 15μ	Thermistor	1000 cycle/ sec	N/A	Two channel 5, no optics
Thermo-graph	5° x 20°	1.8 - 15μ	Thermistor	50 sec/ picture	N/A	Produces photo-graphic record of IR background

Page 104 deleted

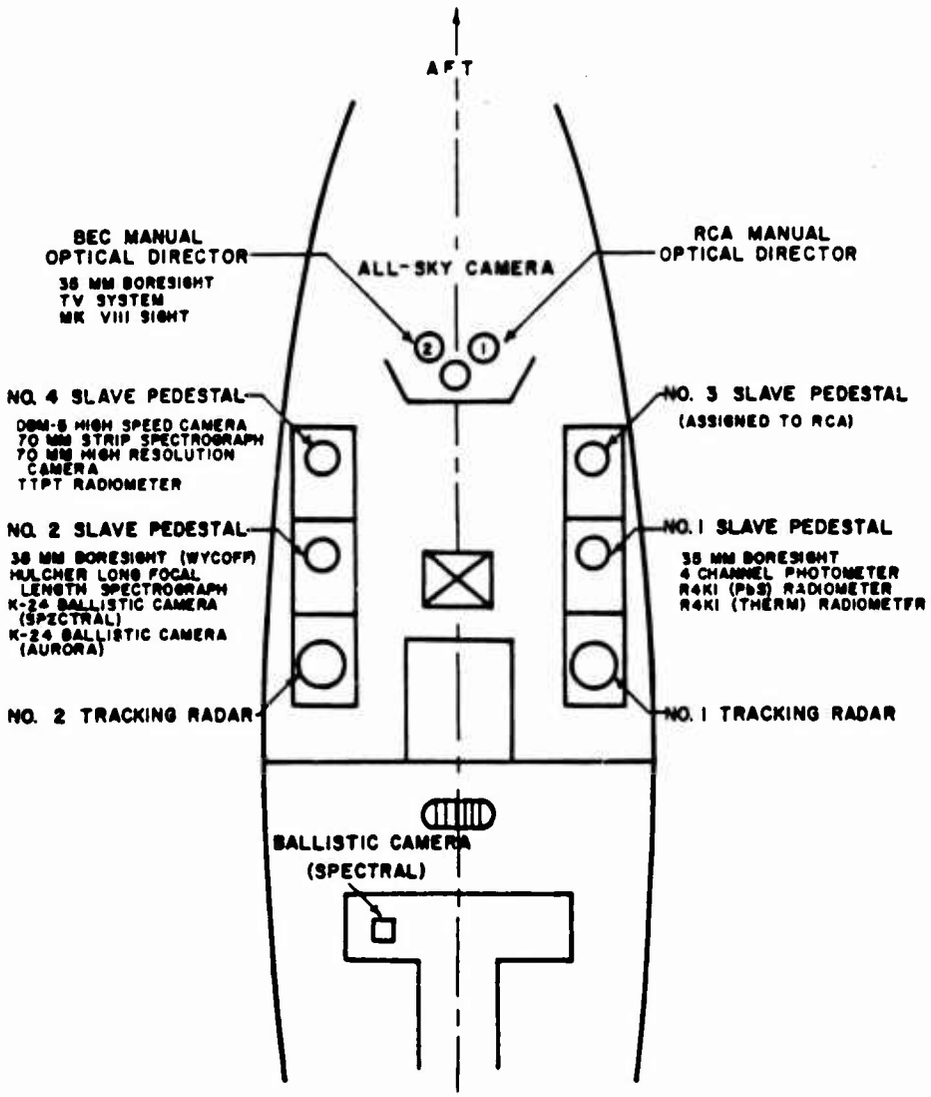

Figure 5.2 Instrumentation layout, DAMP ship.

CHAPTER 6

RESULTS

6.1 STAR FISH PRIME

6.1.1 Burst Measurements. Inclement weather prevented the gathering of satisfactory data in support of pretest objectives. Photographic instrumentation recorded an opalescent background produced by a dense layer of clouds uniformly illuminated by the burst. Burst instrumentation was directed to the point of detonation by Optical Director No. 2. The following descriptions are those of data obtained by each burst instrument.

The 70mm high-resolution camera started 10 seconds prior to burst and operated for 60 seconds. Data were recorded from H - 0 to H + 0.3 second and consisted of 10 frames of evenly exposed, unimaged intensities. At H - 0 the frame containing the burst was totally opaque, and each successive frame became less dense with time.

The 16mm DBM-5 high-speed camera was started 10 seconds prior to detonation and operated for 37 seconds. Data were recorded from H - 0 to H + 0.01 second, and consisted of 4 frames of evenly exposed, unimaged intensities. At H - 0 the frame containing the burst was totally opaque, and each of the three successive frames became less dense

with time.

The 70mm streak objective spectrograph was started 10 seconds prior to detonation and operated for 39 seconds. Burst data were recorded from H - 0 to H + 4 seconds and consisted of a 48-foot length of dense exposed film. The remaining length of film decreased in density with time.

The TTPT Radiometer—Channel A and Channel B—was started 120 seconds prior to H - 0. This instrument was operated until H + 379 seconds during which time Channel A recorded a pulse width of 0.5 msec with an amplitude of 4 volts, and Channel B recorded a pulse width of 0.2 msec with an amplitude of 0.5 volt. Both pulses were recorded at H - 0, and their amplitudes decay with time. Although highly attenuated by dense clouds, results from this instrument are tentatively positive.

The 35mm flight research Wycoff camera was started 10 seconds prior to detonation and operated for 200 seconds. The results were expected to be similar to the 70mm high-resolution camera.

6.1.2 Long-Term Measurements. A long-term period of surveillance was conducted in support of the pretest objectives. However, inclement weather resulted in a serious degradation of recorded information. This

with time.

The 70mm streak objective spectrograph was started 10 seconds prior to detonation and operated for 39 seconds. Burst data were recorded from H - 0 to H + 4 seconds and consisted of a 48-foot length of dense exposed film. The remaining length of film decreased in density with time.

The TTPT Radiometer—Channel A and Channel B—was started 120 seconds prior to H - 0. This instrument was operated until H + 379 seconds during which time Channel A recorded a pulse width of 0.5 msec with an amplitude of 4 volts, and Channel B recorded a pulse width of 0.2 msec with an amplitude of 0.5 volt. Both pulses were recorded at H - 0, and their amplitudes decay with time. Although highly attenuated by dense clouds, results from this instrument are tentatively positive.

The 35mm flight research Wycoff camera was started 10 seconds prior to detonation and operated for 200 seconds. The results were expected to be similar to the 70mm high-resolution camera.

6.1.2 Long-Term Measurements. A long-term period of surveillance was conducted in support of the pretest objectives. However, inclement weather resulted in a serious degradation of recorded information. This

surveillance consisted of mapping an area surrounding the burst point, the conjugate point, and large azimuth and elevation scan patterns covering the operational limits of the optical director and the instrumented slave pedestals.

Post-mission mapping was started at H + 323 seconds and continued intermittently until sunrise on D + 1 day. The sampling periods were taken every half-hour with a duration of from 5 to 10 minutes. A 5-minute final mapping mission was conducted after sunset on D + 1 day.

During the mapping periods, almost total cloud coverage persisted. No auroral phenomena were observed at any time. In addition, no long-term effects were believed to have been recorded which could be directly attributed to the nuclear detonation. It is significant to note that little, if any, long-term effects were recorded in the monitored wavelength regions. In this respect, the severe attenuations imposed on the selected wavelength regions by intermittent precipitation and heavy cloud coverage must be considered. Individual instruments with their preliminary results are listed below:

R4K-1 Thermistor Radiometer. The results from this instrument are unknown due to low levels of recorded signal, but results are believed to be negative.

R4K-1 Lead Sulfide (PbS) Radiometer. The results from this instrument are unknown due to low levels of recorded signal, but the results are believed to be negative.

4-Channel Photometer. The results from this instrument are unknown due to low levels of recorded signal, but results are believed to be negative.

35mm Boresight camera (Slave Pedestal 1). Due to heavy rains, this camera was started after burst at H + 447 seconds and stopped at H + 1245 seconds. No positive results were obtained.

After burst, the thermograph and star camera were directed at the detonation point by the operator. Four thermograph exposures and a sequence series of 3-star exposures for each thermograph exposure were made. The results were negative.

35mm Boresight camera (Optical Director 2). This camera was not operated due to the lack of recordable optical phenomena.

The all-sky camera was operated for Stanford Research Institute and the film delivered to that organization for review. Recording commenced prior to Thor lift-off and ceased at sunrise on D + 1 day.

6.1.3 Support Instrumentation. Eight K-19 aerial ballistic cameras were mounted on Johnston Island to record optical flare data from the Speedball probes. These probes ejected 14 flares at designated points along the trajectory. Positive results were obtained from four of the eight K-19 cameras.

Because of total cloud coverage, the K-24 ballistic (probe) camera mounted on the DAMP Ship yielded negative results with respect to flare data.

6.2 CHECK MATE

A cloud cover estimated at 50 percent obscured the detonation area from the ship. As a result, no direct data was obtained on the burst itself. Data was obtained, however, on the radiation scattered by the intervening atmosphere and the later time debris and/or aurora as it emerged from behind the cloud. The time coverages of those instruments which collected data are shown in Figure 14.1 of Volume 3.

The long-term measurement (background) instruments were initially directed 90 degrees from the burst area in order to prevent direct observation of the burst. They were then directed to the burst area at about H + 25 seconds and commenced the mapping of visible phenomena. The initial data recorded is that radiation emitted by the weapon debris and scattered into the instruments by the atmosphere. Two photometer channels recorded this as shown in Figures 14.2 and 14.3 of Volume 3. The two long-wave photometer channels recorded only a surge at H - 0, and their records need not be included. The

radiation decay as observed by the scattered signals would correspond to the decay of the total weapon complex as it is dispersed. Due to the complete uncertainty of the optical path length from target to instrument, no quantitative values can be attached to the radiating source. The scattered radiation as recorded by the lead sulphide radiometer is shown in Figure 14.4 of Volume 3.

After this period of observing the scattered radiation, the pedestals were directed to the area of the burst. Signals were recorded, but definite photographic boresight records identified a target only after H + 55 seconds, this being the debris resulting from the detonation. Spectral brightnesses as measured by two photometers are shown in Figure 14.5 of Volume 3. (The long-wavelength photometers recorded little or no signals in this time interval and are not included. These data will be further discussed later in this report. In addition, short wavelength signals were recorded out to about H + 7 minutes. However, due to the cloud cover and the fact that no boresight records are available to define the source, they are not included here.) The records are better understood when a description of the debris is given as shown in Figure 14.6 of Volume 3. This is a 45-second exposure beginning at

H + 295 seconds. The camera used for this exposure had a 7-inch, f/2.5 Aero-Ektar lens, a 40-degree x 40-degree field-of-view and used Tri-X Aerecon film. Superimposed on this is a grid of celestial azimuth and elevation angles as viewed from the ship. It must be determined from a comparison of data which were not obscured early by clouds whether the streamers noted in Figure 14.6 of Volume 3 are true aurora (air excited by the passing of fission products) or weapon debris that has become field aligned.

6.3 BLUE GILL TRIPLE PRIME

This test was a major contribution to the significant data recorded during the Fish Bowl series. Figure 14.1 of Voume 4 shows the data coverage. Its [redacted] detonation altitude resulted in backgrounds of considerable magnitudes and durations significant to any evaluations of passive optical detection systems.

Detonation occurred at 09:59:48.5 GMT, [redacted] At this time the instruments viewed the burst point [redacted] A cloud obscured the burst point, but as the fireball expanded and rose, a full view was afforded of the event. Figure 14.2 of Volume 4 is a

series of photographs obtained from the K-24 spectral camera zero order which shows the fireball history. Figure 14.3 of Volume 4 shows selected frames from the 35mm boresight on Pedestal 1 and clearly shows the incandescent debris cloud and toroid. The operator was intentionally scanning across the fireball, toroid, and surrounding area, hence the target moves around considerably. The photometers and radiometers measuring the background levels were slaved to this operator.

At detonation the photometric and radiometric instrumentation were viewing a point approximately 90 degrees away, in azimuth, from the burst point and recorded the indirect, scattered radiation at this point. Figures 14.2, 14.3 of Volume 3, and 14.4 of Volume 4 show the photometric levels recorded, and Figure 14.4 of Volume 3 shows the lead sulphide infrared levels. All are characterized by a rapid return to background level. The radiation levels at 8826 Å were insufficient to be recorded, with the exception of a sharp transient spike at H - 0.

During the interval in which the sensitive instruments were directed away from the burst area, the instruments positioned on the stabilized platform were viewing the event directly. The composite photograph mentioned above was

recorded from this pedestal, and excellent data were also recorded by the 35mm boresight camera equipped with the triple layer emulsion XR film.

Densitometric scans were made of selected frames of the XR emulsion boresight record to show the background decay at some angular separation from the fireball. Figure 14.5 of Volume 4 shows the results. Only the background above the burst could be measured because of cloud obscuration beneath and to the sides of the burst point. It was also difficult to precisely find the center of the burst at these times, and it was more constructive to measure the background above the fireball edge. The background decay is very apparent in the graph.

Additional points were read at selected times for a point approximately 10 degrees from burst center and these are shown in Figure 14.6 of Volume 4. Shown also, but to be discussed below, are King Fish data. It can be seen that the background, 10 degrees above the burst as recorded by this emulsion, returns to essentially pre-burst levels in slightly less than one minute. By approximately 1½ minutes, the fireball and debris sphere have degenerated into the toroid.

At approximately H + 50 seconds the photometer and radiometers were positioned on the debris sphere proper and the recording of brightness commenced. Exceptionally strong radiation levels were recorded for the incandescent sphere and are shown in Figures 14.7 and 14.8 of Volume 4 for the four photometers. The oscillations present are the result of brightness variations observed during the mapping period. Figure 14.9 of Volume 4 shows the area of the sphere covered by the photometers.

Of the radiometers, only the PbS instrument recorded significant data during this test. During the debris sphere mapping period, saturation occurred, and it was not until the toroid formed that signals were readable; as a result, radiometric data of the debris are not available. Figure 14.9 of Volume 4 also shows the sphere area covered by the radiometer. After degeneration of the debris into the toroid, the mapping data were quite erratic in nature as a result of the varying toroid brightnesses and incomplete field coverage. It is constructive, therefore, to present the photometric data as envelopes defined by the maximum and minimum data points. These are shown in Figures 14.10 through 14.12 of Volume 4. Figure 14.13 of Volume 4 is for the radiometer not given as an envelope.

In addition to the photometric, radiometric, and photographic brightness data presented above, significant data were obtained by the XR emulsion related to fireball dynamics. Measurement of the fireball and toroid diameters gave a rate of fireball growth, toroid growth, and altitude. Figure 14.14 of Volume 4 shows the fireball and debris sphere growth up to that time when the toroid was formed.

6.4 KING FISH

Like Blue Gill Triple Prime, this test was a primary contributor to the data obtained from Fish Bowl. In contrast to Blue Gill Triple Prime, this test were noticeably shorter.

Detonation occurred at 12:10:06 GMT Figure 14.1 of Volume 5 shows a photographic record of the burst;

Figure 14.2 shows the data coverage. As described above, the instruments during detonation recorded scattered radiation backgrounds. For the photometers, these are shown in Figures 14.2 and 14.3 of Volume 3. For the PbS radiometers, these are shown in Figures 14.4 of Volume 4, 14.3 of Volume 5, and 14.4 of Volume 3.

Densitometric scans were made of the fireball and adjacent areas. For this test it was convenient to scan horizontally across the fireball rather than vertically as on Blue Gill Triple Prime. Figure 14.4 of Volume 5 shows the results for selected frames. The center of the burst was easily positioned on the film, and all scans were normalized to that point. A significant background difference is observed between this test and Blue Gill Triple Prime.

Figure 14.6 of Volume 4 shows the photographic background and fireball-debris decay, obtained from the XR emulsion as described above. The King Fish background 10 degrees from the burst lasts for 5 seconds in comparison to 45 seconds from the Blue Gill Triple Prime, and the fireball persists for less than 35 seconds in comparison to 95 seconds for Blue Gill Triple Prime.

The fireball was acquired at H + 12 seconds, and immediately photometric and radiometric data were recorded.

These are shown in Figures 14.5 and 14.6 of Volume 5, respectively. The areas of the fireball mapped by the instruments are shown in Figure 14.9 of Volume 4. Unlike Blue Gill Triple Prime, the fireball of this test was transparent, not opaque, and the internal debris structure could be observed. Also, a markedly more rapid decrease in brightness was observed.

Measurements of the rate of growth of the fireball very quickly show the effect of burst altitude on fireball dynamics. Figure 14.14 of Volume 4 is a time plot of diameter of the fireball proper, horizontal luminous shock, and vertical luminous shock. Figure 14.1 of Volume 5 shows these shocks.

Very definite aurora were observed on this test, and photometric brightnesses were recorded for three wavelengths. These are presented in Figure 14.7 of Volume 5. The strong signals in the two short-wavelength photometers are attributed to the nitrogen second positive and/or ionized nitrogen molecular radiation and the 8826 Å signals possibly from the nitrogen first positive molecular radiation. Cloud cover developing shortly after formation of the aurora prevented the extensive mapping and long-term photography that was possible on Check Mate.

6.5 TIGHT ROPE

H - 0 occurred at 07:30:00 GMT. The low altitute resulted in considerable fireball confinement.

As a result of the instruments viewing more closely to the burst area, excessively strong radiation levels were experienced by the photometers. Figure 14.1 of Volume 6 shows the data coverage. Brightness values for the 7000 Å and 8826 Å photometers are shown in Figures 14.4 of Volume 4 and 14.3 of Volume 5; the short wavelengths instruments were saturated. Until approximately H + 25 seconds, the data were random because of erratic

pedestal pointing; at this time the burst area was acquired and mapping started. The fireball by this time had degenerated into a toroid similar to that observed on Blue Gill Triple Prime, and all subsequent data are of it. Figures 14.2 and 14.3 of Volume 6 show the decay envelopes for 3892 Å and 4036 Å. The 8826- and 7000-Å photometer returned to background in approximately 45 seconds. Severe saturation resulted on the PbS radiometer for nearly two minutes after H - 0. A few unsaturated points were obtained but are not useful independently. The general brightness level after two minutes was 4×10^{-8} watts-cm^{-2}-Ω^{-1}-$\Delta\lambda^{-1}$, hardly above the pre-burst background of 2×10^{-6}.

Toroid diameter growth rate was determined from bore-sight film measurements. The altitude of the fireball and toroid remained nearly constant.

CHAPTER 7

DISCUSSION

7.1 STAR FISH PRIME

7.1.1 Burst Measurements. The major objectives for this portion of the experiment were not achieved due to inclement weather. Persistent cloud coverage (100 percent) and heavy rain were experienced during the burst equipment recording periods. An intense opalescent background was photographically recorded at detonation. Uniformly exposed frames of film, which varied in density corresponding to prevailing intensity during the dwell period immediately following detonation, were also recorded. The TTPT radiometer appeared to have recorded little useful data due to the opacity and severe attenuation imposed by the dense cloud layer. The TTPT signals which were recorded on both radiometers were extremely short in pulse duration and were of low amplitude. The unsatisfactory results can be directly attributed to the great amount of absorption in the monitored wavelength region.

7.1.2 Long-Term Measurements. Inclement weather persisted throughout the majority of the postdetonation mapping exercise. Again, weather was the major deleterious factor affecting the achievement of the objective during

this time frame. Postdetonation mapping was scheduled to commence within seconds after detonation; however, this could not be accomplished due to heavy precipitation which would have damaged the instrumentation had the protective covers been removed. Mapping commenced at approximately H + 5 minutes and continued on an intermittent basis until sunrise on K + 1 day. Due to the continued negative results, active participation was terminated. On a long-term basis, radiometric and photometric charts show that little, if any, measurable data were recorded in respect to monitored wavelength regions. However, this fact is indeed significant, because the severe attenuation and absorption cannot be ignored. It tentatively appears that little information will result from the monitoring of the associated long-term effects. No optical phenomena or auroral displays were observed or recorded which could be directly attributed to the nuclear detonation.

7.1.3 Support Findings. Support instrumentation was utilized to record optical flare images from fourteen optical flares ejected from the three 6.13 Speedball probe vehicles at specified points along the probe trajectory. Primarily, the flare images will be used for optical correlation with the RF experiments. It appears that

certain flares were recorded by the K-19 cameras on each of the three Speedball flights. Flare images could not be located on the K-24 film record. Lack of images on the K-24 film can be directly attributed to the dense cloud coverage during the three Speedball flights.

7.2 CHECK MATE

The early time cloud obscuration of the burst area limited the optical experiments on this test to photographic and photometric measurements of the aurora-debris formation.

As it was believed that the artificially produced aurora would create a measurable background, the choice of photometer spectral sensitivities was predicated primarily upon presence of molecular nitrogen emission common to aurora. One short wavelength instrument was selected to detect the λ3914 Å (0,0) bandhead of N_2+, the other short wavelength instrument was to measure a clear region of the band system at 4030 Å. There is also nitrogen second positive radiation overlapping the N_2+. It is not possible to distinguish between the two with the 100-Å bandpass. One long wavelength channel was to measure the (1,0) band of the nitrogen first positive system at λ8912 Å and the other a clear region of that system at λ7000 Å. All bandwidths were nominally 100 Å. The interference filter for the λ8912-Å channel was actually centered λ8826 Å and thus was positioned between the (1,0) and (2,1) bands of the nitrogen first positive system. It was anticipated that an intensity and/or lifetime difference would be detected between the two

different nitrogen systems.

The 35mm boresight record for pedestal 1 was used to ascertain those times when the photometers were scanning the streamer-like formations. Figure 14.5 of Volume 3 indicates those times when the 1-degree circular fields of view of the photometers were partially or fully filled. A tabular summary of the data is shown in Table 7.1. The long wavelength data were very slightly above threshold signal of the photometers and therefore are not graphically presented.

It was suggested in information released at the Optical Measurements Symposium, Operation FISH BOWL, sponsored by DASA held March 12, 13, 14, 1963, Bedford, Massachusetts, that the effect resembling auroral streamers (see Figure 14.6 of Volume 3) is really detonation debris that has become aligned with the magnetic field lines. If this is the case, then the photometric data presented above are not applicable to aurora intensities. A spectrum of the emission from these streamers is not available to resolve this point.

7.3 BLUE GILL TRIPLE PRIME

Blue Gill Triple Prime test exhibited radiation backgrounds of the longest duration, which are of particular interest to any discussion of discrimination techniques. It was shown in Figures 14.10 through 14.12

of Volume 4 that the recordable background persists for as long as one hour after burst in the 4000-Å region of the spectrum and for as long as 2½ minutes in the lead sulphide infrared. The 7000- to 8000-Å wavelengths returned to background within ten minutes. It is obvious that the shorter wavelength visible region of the spectrum would be a particularly undesirable choice for discrimination instrumentation. The rapid return of the infrared background suggests that the effects of a precursor burst of the characteristics of Blue Gill Triple Prime would not be as effective as initially concluded.

The relatively low altitude of burst resulted in considerable fireball confinement and the formation of a spherical, incandescent, debris cloud which persisted for approximately 1½ minutes. During this period the radiation levels were in excess of the pre-burst backgrounds by the following amounts:

	Debris Sphere ($watts \cdot cm^{-2} \cdot \Omega^{-1} \cdot Å^{-1}$)	Pre-burst Backgrounds ($watts \cdot cm^{-2} \cdot \Omega^{-1} \cdot Å^{-1}$)
λ 3892 Å	1×10^{-9} - 7×10^{-8}	5.8×10^{-12}
λ 4036 Å	2×10^{-10} - 8×10^{-9}	1.6×10^{-10}
λ 7000 Å	2×10^{-9} - 5×10^{-8}	3.8×10^{-10}
λ 8826 Å	5×10^{-8} - 9×10^{-8}	5.0×10^{-10}

The pre-burst backgrounds are those measured immediately prior to burst, in a general area 90 degrees away (in azimuth) from the burst point. These values are those measured approximately 1 second prior to burst; values obtained during pre-mission mapping are not significantly different from these. It is possible, and expected, that the ambient backgrounds, that is, those not attributed to the burst, would vary from those quoted. The infrared data show steady return to pre-burst magnitudes and attain equilibrium in approximately H + 2 minutes. During the last minute, the toroid was the prime contributor of the data; when the toroid was not completely filling the field of view, background levels were at or near the pre-burst values, indicating that, slightly away from the burst area, infrared backgrounds would be negligible.

The data recorded for this test are evidence that, up to approximately 45 seconds after detonation, the fireball and debris cloud would seriously affect radiometric and photometric detection capabilities. Additionally, the toroid would contribute to the background radiation for nearly 30 minutes after detonation. It is to be understood that the above statements apply only to the immediate burst area.

7.4 KING FISH

The King Fish data are very significant when considered with those obtained on Blue Gill Triple Prime, for the altitude effects on burst radiation magnitudes, lifetimes, and burst dynamics are clearly evidenced.

Also markedly different are the fireball diameters and altitude increases at any given time after detonation.

The atmospheric density at King Fish burst versus of Blue Gill Triple Prime, unquestionably was the major contributing factor to the differences in the two tests.

It can be seen in Figure 14.1 of Volume 5 that the fireball rapidly becomes transparent, and excellent observation of the debris expansion is noted. Measurements of these data on the K-24 spectral camera indicate a debris expansion rate of nearly 2.3 kilometers per second. Another interesting debris phenomenon observed was

a strong radiator at λ6700 Å. This is shown in Figure 7.1. The species of this radiation is concluded to be Lithium (λ6707 Å, 2s-2p transition). This appeared to be the only atomic spectral radiation and was superimposed on a continuum.

7.5 TIGHT ROPE

Few significant data were obtained from this test as a consequence of inaccurate pedestal direction and instrument saturations. As indicated in Figures 14.2 and 14.3 of Volume 6 close similarity with Blue Gill Triple Prime is observed in the background radiation decay. The yields were markedly different as well as the altitudes, and additional data are thus presented showing the altitude-yield influence on radiation magnitudes and durations.

TABLE 7.1 CHECK MATE DEBRIS SPECTRAL BRIGHTNESS, WATTS · CM^{-2} · Ω^{-1} · $Å^{-1}$

TIME SECONDS AFTER H-O	λ, Å 3892	λ, Å 4036	λ, Å 7000	λ, A 8826
70*	8.0×10^{-11}	3.6×10^{-11}	7.6×10^{-10}	3.3×10^{-8}
82.5+	8.0×10^{-11}	5.6×10^{-11}	7.6×10^{-10}	3.2×10^{-8} #
104*	8.4×10^{-11}	4.5×10^{-11}	7.6×10^{-10}	3.3×10^{-8}
BACKGROUND→	1.4×10^{-11}	2.5×10^{-12}	6.6×10^{-10}	3.18×10^{-8}

* FIELD OF VIEW NOT COMPLETELY FILLED

\+ FIELD OF VIEW IS COMPLETELY FILLED

\# MINIMUM BRIGHTNESS DISCERNIBLE

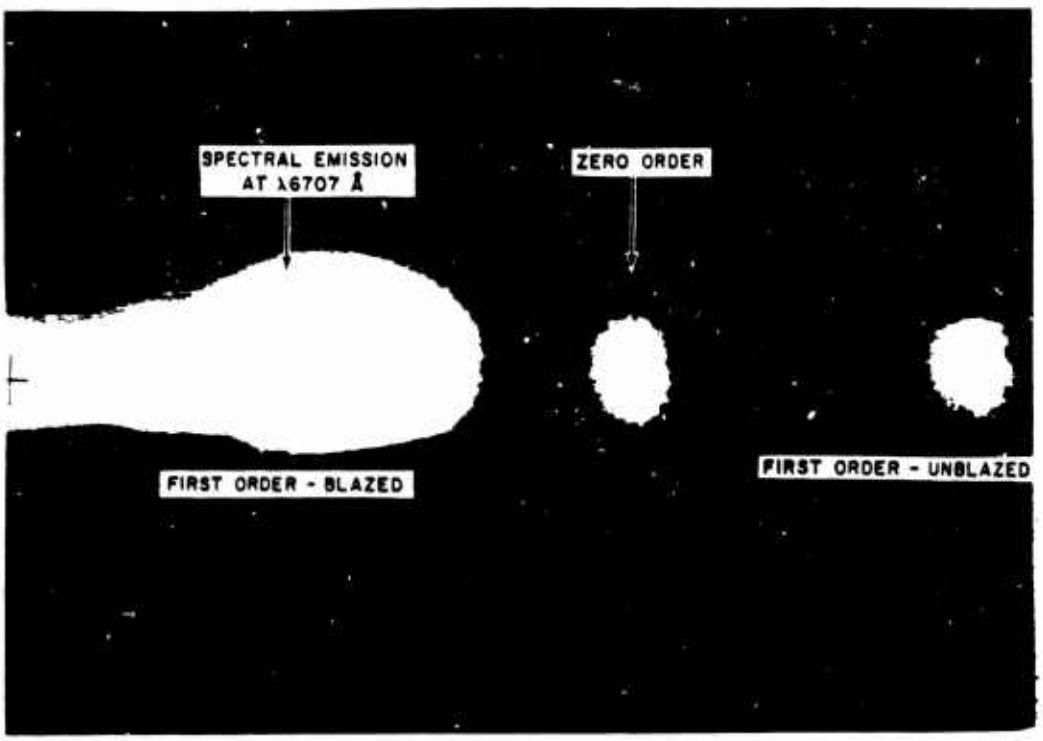

Figure 7.1 Spectrum of King Fish debris at H+2.4 seconds.

CHAPTER 8

CONCLUSIONS

A primary objective of the DAMP operation in Fish Bowl was the measurement of the background radiation levels produced by nuclear radiation magnitudes, lifetimes, and spectral distributions. It is concluded that these objectives were generally realized.

Both the magnitudes and lifetimes of the backgrounds have been measured and presented; primarily, these were for Blue Gill Triple Prime and King Fish, but together they define bounds. King Fish exhibited the shortest lifetime of the tests, Blue Gill Triple Prime and Tight Rope the longest. The data for Check Mate were not sufficient to indicate its lifetime, but the [ ] altitude unquestionably affected the lifetime, [ ] It is difficult, however, to define the magnitudes of radiation because, generally, the instruments saturated before the backgrounds peaked. For Star Fish Prime, no accurate data was gathered due to inclement weather throughout the day of the test.

Spectrally, it was shown that the lead sulphide infrared data was not significantly above background after approximately two minutes for any test. It should be noted that

the radiometers were operating in a total chop mode, not the conventional reticle chop used on reentry measurements, and correlation of burst and reentry data is difficult. No significant data were recorded by the thermistor (1.8μ to 15μ) radiometer. An attempt at approximating the temperature of the fireball of King Fish and the debris sphere of Blue Gill Triple Prime was made using the photometric and radiometric data. A gross disparity was noted between the infrared and visible data magnitudes, and the conclusion was that the targets did not radiate as a grey-blackbody. The photometric data suggest a target temperature of nearly 3000°K while the infrared data suggest a temperature of approximately 300°K.

In the visible-optical wavelengths, significant data were obtained showing considerable backgrounds in the violet-blue region, presumably from the aurora radiation. The beta particles that create aurora follow the magnetic field lines; as a consequence of the ship position, the instruments viewed the aurora cross-sectionally, which made photographic observation difficult. Johnston Island data presented at the Optical Symposium showed considerable aurora on Blue Gill Triple Prime immediately following detonation and, although not recorded photographically from the DAMP

ship, they were very likely detected photometrically. There is also a very strong probability that the streamers emanating from the fireball in Figure 14.2 of Volume 4 are aurora and not an optical-film effect.

No short-time spectra of the fireballs were obtained, but some spectra were obtained of the debris cloud on King Fish, and a strong radiator was lithium. This species radiator was also briefly observed on Blue Gill Triple Prime K-24 ballistic camera spectral records. The origin of the radiation cannot be determined from the available data, but the presence of lithium in a fusion device is to be expected.

The measurements of fireball, debris, sphere, and toroid growth have added to the previously available data. These data are shown in Figure 8.1. Here, too, the altitude influence on dynamics is observed.

Page 136 deleted.

REFERENCES

1. "Report on Nuclear Interference"; Advanced Research Projects Agency, Institute for Defense Analysis, Washington, D.C.; IDA ARPA TR 60-3; Secret Restricted Data.

2. "Passive Radiation Countermeasures Feasibility Studies," Task II Summary Report, Part II PRCM-T2F - Part II SON2-58058/27, 31 December 1961; Hughes Aircraft Company.

3. "Operation Fish Bowl Technical Summary," Special Report No. 6, 19 November 1962; DASA Data Center, General Electric TEMPO, Santa Barbara, California.